

Universität für Bodenkultur, Wien
Department für Wald- und Bodenwissenschaften
Institut für Bodenforschung

University of Natural Resources and Life Sciences, Vienna
Department of Forest and Soil Sciences
Institute of Soil Research



Where do roots leak phosphorus?

An Inquiry on Root Phosphorus Efflux into the Rhizosphere

Master Thesis

Mag.phil. Rainer Franz Mühlbacher, BSc.

Supervised by

Univ.Prof. DI Dr.nat.techn. Walter Wenzel

DI Dr. Jakob Santner

Vienna and Tulln/Donau, April 2015

Table of Contents

ABBREVIATIONS	5
1. INTRODUCTION	6
1.1. Background	6
1.1.1. Phosphorus in soils	7
1.1.2. Phosphorus in the rhizosphere	9
1.1.3. Apoplastic vs. symplastic P uptake	10
1.1.4. Transmembrane transport in plants	11
1.1.4.1. Michaelis-Menten kinetics	12
1.1.4.2. Phosphorus efflux	13
1.1.4.3. P-efflux and the Michaelis-Menten model	15
1.1.5. Long distance transport of phosphorus in plants	17
1.1.6. Xylem and phloem loading and unloading	17
1.2. Objectives	19
2. MATERIAL AND METHODS	20
2.1. Growth media	20
2.1.1. Soil.....	20
2.1.2. Agarose gel	21
2.2. Diffusive gradients in thin films technique – DGT	22
2.2.1. Function	22
2.2.2. DGT gel preparation	23
2.3. Colorimetric determination of P	24
2.4. ³¹ P-efflux experiments	25
2.4.1. DGT sampling setup.....	26
2.4.2. Preparation of DGT standards for laser ablation ICP-MS.....	27
2.4.2.1. Assembly of DGT samplers	27
2.4.2.2. Loading of the DGT standards	28
2.4.3. Laser ablation ICP-MS.....	30
2.5. ³³ P-efflux experiments	31
2.5.1. Preliminary experiments	31
2.5.2. Main experiments	34
2.5.2.1. Main experiments with soil rhizotrons.....	35
2.5.2.2. Main experiments with agarose rhizotrons.....	35
2.5.3. Relative root efflux analysis	36
2.5.3.1. Image calibration for relative efflux analysis.....	36
2.5.3.2. Analysis of root axis/root tip ratio	37

3. RESULTS AND DISCUSSION	39
3.1. ³¹ P-efflux experiments	39
3.1.1. DGT standards for laser ablation ICP-MS.....	39
3.1.2. Calibrated and scaled DGT pictures.....	40
3.2. ³³ P-efflux experiments	42
3.2.1. Preliminary experiments.....	42
3.2.2. Soil Forchtenstein	44
3.2.2.1. With phosphorus fertilization	44
3.2.2.2. Without phosphorus fertilization.....	44
3.2.3. Soil Santomera.....	45
3.2.3.1. With phosphorus fertilization	45
3.2.3.2. Without phosphorus fertilization	46
3.2.4. Gelrite/agarose gel	47
3.3. Root axis to root tip efflux ratios	49
3.3.1. Image calibration: grey values vs. ³³ P-activity.....	49
3.3.2. Analysis of root axis/root tip efflux ratio	51
3.4. Discussion	52
3.4.1. ³¹ P-efflux experiments.....	52
3.4.2. ³³ P-efflux experiments.....	52
3.4.2.1. Experiments with soil.....	52
3.4.2.2. Experiments with agarose media	54
3.4.3. Root axis to root tip efflux ratios	55
4. CONCLUSION	56
5. REFERENCES	57
6. APPENDIX	59
6.1. Method protocols.....	59
6.1.1. Soil fertilization protocol.....	59
6.1.2. Soil watering protocol	60
6.1.3. LA-ICP-MS standard preparation protocol	61
6.1.4. Hydroponics/Gelrite nutrient solution protocol	62
6.2. Calibration tables for the ³¹ P-efflux experiments.....	63
6.3. List of rhizotrons for the ³³ P-efflux experiments	67
6.4. Tables of root axis/root tip efflux ratios	70

Acknowledgements

Firstly my thank goes to Jakob Santner. This master thesis is not imaginable without his fundamental research idea, his experimental ideas and his profound and competent help throughout the whole work and the many, many problems appearing during the experimental phase. He always knew the way out. Without his guidance on the one hand, but also without the freedom he gave me while working, I would have been lost either scientifically or concerning my motivation. His vivid spirit and always optimistic and pragmatic troubleshooting behavior is truly exemplary.

Secondly I want to thank Walter Wenzel who not only was the one to place me with Jakob and his idea initiating this thesis and the whole RHIZO working group, but who always showed interest in the progress and who always encouraged the project. He is the father of this project and the RHIZO group in its very best meaning.

Special thank also goes to Andreas Kreuzeder and Christoph Höfer, who helped in parts of this thesis and provided knowledge. Andi in particular did a great job in the relative quantification of the root efflux with his diverse software skills. Chris was a great help concerning especially the evaluation of the LA-ICP-MS data, not at least with the evaluation file he programmed for this purpose.

Further thanks go to the whole RHIZO working group. There was always a great team spirit and I found many open ears when sitting at lunch or having a nice coffee in the “terrarium”. The amicable atmosphere among the master students not only in the respectable halls and laboratories of the institute in Tulln, but also and especially outside of it were and are a great enrichment of my life. A burden shared is a burden halved.

Not the least I want to thank Alexandra, who never complained as I grizzled when problems arose, or when I told her about the project in a most detailed way, again and again.

Also my parents have to be named here. They never lost faith in me and encouraging words never dried up throughout my certainly long student career.

Abstract

Phosphorus is of particular importance in plant nutrition. As P-fertilizers have to be made from declining workable rock phosphorus deposits, P dynamics in the soil and in the rhizosphere are of great agricultural interest. Uptake kinetics is an essential aspect in this context. Studies conducted in the 50s and 70s of the 20th century resulted in adaptations of the Michaelis-Menten enzyme kinetics model as an uptake kinetics model also taking into account a certain threshold below which no phosphorus uptake can occur due to efflux exceeding influx. After findings of phosphorus hotspots within the rhizosphere of rape seed plants using diffusive gradients in thin films technique (DGT) ferrihydrite gels and laser ablation inductively coupled plasma mass spectrometry a possible connection between root phosphorus efflux and those hotspots was hypothesized.

Here those experiments were repeated with maize plants. Additionally, to establish proof for the hypothesized connection, a series of experiments using radiophosphorus and digital autoradiography was carried out. Maize seedlings grown in P-fertilized and non-fertilized acidic and alkaline soils as well as in agarose gels were labeled with ³³P and DGT strips were applied for a period of 48 hours. After this the DGT strips were removed from the root surface and exposed to autoradiography screens for 48 hours and scanned afterwards.

The experiments resulted in the detection of phosphorus hotspots in the rhizosphere of maize plants and in clear evidence that phosphorus in the rhizosphere is released by the plant roots in a spatially very heterogeneous way. Phosphorus efflux mainly occurs at the root tips whereas efflux along root axes is very small. Overall mean relative quantification of root phosphorus efflux shows a mean axis-to-tip ratio of 0.003, *i.e.* only 0.30% of total efflux occurs along main axes. Results of the acidic soil show ratios of about 0.004 in non-fertilized and 0.012 in P-fertilized treatments; results of the alkaline soil show ratios of about 0.003 in non-fertilized and about 0.004 in P-fertilized treatments. There are no indications that the results are biased by artifacts such as root injuries, the zero-sink qualities of the DGT gel as a sampling device, or microbes as the source of phosphorus hotspots.

According to clear evidence obtained by the experiments, efflux quantifications relating to root mass, root surface area, root length, etc. are inappropriate and future quantifications should relate mainly to root tips. We show that the Michaelis-Menten model as it has been

applied in previous studies is inaccurate as it describes uptake rates for the entire root system where (almost) only root tips should be taken into account.

Abbreviations

- ATP: adenosine triphosphate
- Ci: Curie, a non-SI unit of radioactivity, defined as $1 \text{ Ci} = 3.7 \times 10^{10}$ decays per second
- c_{min} : lowest soil solution concentration at which net ion uptake can occur
- CPM: unit for radioactive decay as counts per minute, signal intensity in counts per minute
- DGT: diffusive gradients in thin films
- DNA: deoxyribonucleic acid
- GMP: guanosine monophosphate
- GTP: guanosine triphosphate
- LA-ICP-MS: Laser Ablation Inductively Coupled Plasma Mass Spectrometry
- MES: common name for the buffer 2-(*N*-morpholino)ethanesulfonic acid
- mRNA: messenger RNA, family of RNA molecules conveying information from DNA to the ribosome
- P: phosphorus (^{31}P)
- ^{32}P , ^{33}P : the two radioisotopes of phosphorus
- PHT[...]: certain type of phosphate transporter, a protein group
- RNA: ribonucleic acid
- tRNA: transfer RNA, physical link between nucleotide sequence of RNA/DNA and amino acid sequence of protein, an amino acid carrier

1. Introduction

Phosphorus is, together with nitrogen and potassium, one of the three major limiting nutrients for the productivity of ecosystems. For life in general and living cells in particular, phosphorus plays an essential role especially in terms of energy conversion systems (ATP), genetic information and evolution (DNA, RNA), phosphorylation-based signaling pathways, and major structural compartments such as cell membranes (phospholipids). Therefore, and because phosphorus cannot be replaced by any other element in those systems, it is an indispensable resource. Phosphorus can be found everywhere in nature, especially in soils and sediments. In soils the largest part of it is immobile and thus not accessible for plants what is of great importance for agriculture. Due to this immobility and its dilution in the environment it has to be regarded as a non-renewable resource that is mined and traded throughout the world for its main use as a fertilizer. As workable phosphorus deposits only provide this resource for a certain period of time and as worldwide demands for it increase due to a growing world population, phosphorus supply is a serious future issue (Marschner and Marschner 2012; Nussaume et al. 2011; Smith et al. 2003; Kreuzeder 2011).

The following sections of this introduction discuss soil-plant phosphorus interactions and the dynamics of phosphorus within plant tissues.

1.1. Background

The process of phosphorus acquisition by plants comprises the transport of phosphorus from the soil to the root surface, the transmembrane transport from the exterior solution into the cell plasma and the symplast, and the long-distance transport from the roots into aerial parts of plants such as leaves or inflorescences and also back down from aerial tissues to the roots. A specific aspect of the transport into the cell plasma is the kinetics of the phosphorus uptake which can be described as protein kinetics or enzyme kinetics, respectively, and the efflux of phosphorus from the roots into the rhizosphere, another specific, yet potentially important aspect of plant P uptake. The following section is treating those aspects.

1.1.1. Phosphorus in soils

Phosphorus is an essential macro-nutrient for organisms in general and thus for plants in particular. Despite the abundance of phosphorus in the environment it is not easily accessible for plants and also not evenly distributed in soils. Among the anionic nutrients phosphate, sulfate, nitrate and chloride, and compared to other major nutrients, phosphate is the least mobile due to its strong adsorption to soil particles – only a marginal proportion of soil phosphorus is plant-available (Bresinsky et al. 2008; Hinsinger 2001). Up to 80% of the phosphorus in soils can be present as organic residues and thus is not directly available for plants which are only able to take up phosphate as H_2PO_4^- and HPO_4^{2-} . However, the vast majority of inorganic phosphorus in the soil is not accessible for plants either. In the process of weathering of soil parent material during pedogenesis, mineral sources of phosphorus dissolve and phosphates are bound by constituents of the clay fraction (oxides, clay minerals), are re-precipitated as secondary minerals (aluminium phosphates, calcium phosphates, and iron phosphates), or are incorporated into humic substances (Blume et al. 2010; Kreuzeder 2011). The most important mineral source for phosphate in the pedo- and the biosphere is apatite, which can be of magmatic or pedogenic origin. Total P contents of soils may vary from $<100 \text{ mg P kg}^{-1}$ in sandy soils such as podsoles in temperate zones, $200\text{--}800 \text{ mg P kg}^{-1}$ in silty, loamy, and clay soils in temperate zones, and about $1000 \text{ mg P kg}^{-1}$ in young soils originating from P-rich basalts and basalt ashes. Agricultural soils that have received high inorganic or organic P-fertilizations over decades may contain about $2000 \text{ mg P kg}^{-1}$ (Blume et al. 2010). It is estimated that about 98% of the soil phosphorus is bound either inorganically or organically and not directly accessible for plants, and that less than 2% are adsorbed to soil surfaces or dissolved in the soil solution (less than 0.1% of total soil P), respectively, and therefore accessible for plants (Schroeder 1972; Blume et al. 2010).

The distribution of P among various P species is mainly determined by solution pH. As plants have their phosphate uptake maximum between pH 5 and 6, the form of acquired phosphate is mainly H_2PO_4^- which is the predominant phosphate species at this pH; at pH 7.2 to 12.0 HPO_4^{2-} is predominant (Blume et al. 2010; Nussaume et al. 2011). Besides free phosphate anions and depending on the solution pH, also Ca-phosphate complexes, such as $\text{CaH}_2\text{PO}_4^-$ and CaHPO_4 , iron and aluminium phosphates and organically-bound phosphates (may vary between 20-70% of total P in solution) can be found in the soil solution. Total concentrations of phosphate in the soil solution range from $1\text{--}100 \mu\text{g P L}^{-1}$ in unfertilized soils

to 100-5000 $\mu\text{g P L}^{-1}$ in A horizons of fertilized soils. Contents of 300-800 $\mu\text{g P L}^{-1}$ are considered optimal for agricultural purpose (Blume et al. 2010). However, phosphate concentrations and thus the availability of dissolved and as such available phosphate in the soil solution are mainly controlled by two different equilibria:

Precipitation-dissolution equilibria: In acidic soils concentrations of Fe- and Al-oxides in the soil solution increase due to their increased solubility; thus trivalent Fe and Al can be found in relatively high concentrations in the soil solution. In neutral and alkaline soils Ca and to a smaller extent Mg are found to be the predominant cations, whereas Fe and Al are negligible. Therefore phosphates will partly precipitate as dicalcium or octocalcium phosphates or as different types of apatite under neutral to alkaline conditions and as iron and aluminium phosphates (e.g. vivianite, strengite, variscite, etc.) under acidic conditions. Again, the solubility of the various P minerals depends on the solution pH (Hinsinger 2001; Nussaume et al. 2011).

Adsorption-desorption equilibria: Adsorption onto and desorption from various soil constituents are major processes that control solution P concentrations; most P species in the soil are negatively charged and therefore are adsorbed to cationic soil constituents. Hence, the most important sorbents are compounds that contain either protonated hydroxyl (Al, Fe oxides), carboxyl (organic compounds), or silanol (clays) groups. In particular metal oxides play an important role for the adsorption-desorption equilibrium; due their high point of zero charge (between pH 7-10) they are positively charged over a large pH range. Additionally they occur as small crystals and therefore have a considerable specific surface area and a high reactivity as sorbents. At decreasing pH values the metal hydroxides show a larger degree of protonation and therefore their capacity to adsorb phosphates increases; when only considering metal oxides, the mobility of phosphates in the soil decreases with decreasing pH. Desorption is mostly based on ligand exchange reactions, therefore lowered phosphate concentrations in the soil solution and raised concentrations of competing anions enhance the desorption of phosphates from soil particles due to the shifted equilibrium. However, metal oxide surfaces and other important soil sorbents such as clay minerals apparently have a higher affinity for phosphates than for competing inorganic (like sulphate or bicarbonate) or organic anions (like carboxylates). Hence, large concentrations of competing inorganic and organic ligands must occur to desorb phosphates from soil sorbents (Hinsinger 2001).

1.1.2. Phosphorus in the rhizosphere

In the rhizosphere, *i.e.* the parts of the soil that are under direct influence of living plant roots, soil P contents and soil solution concentrations are usually different from those in bulk soil. As plants take up water, phosphate dissolved in the solution is taken up by the roots. But this uptake-driven convection (mass flow) of water and solutes in the soil can only provide for a fraction of the phosphorus that is required by plants. As a consequence of the strong sink qualities of plant roots, a steep concentration gradient between bulk soil and rhizosphere is generated, which is the driving force for the diffusion of phosphates towards plant roots (Hinsinger 2001). Diffusion is considered to be the essential way of phosphate transport in soils by means of which 92% of the entire phosphate is transported to the root surface, whereas mass flow comprises of 5%, and the amount of phosphate that is reached by root growth is 3% of the entire phosphate supply of *Zea mays* in a silt loam soil (Barber 1995). Phosphate mobility is impeded by the high tortuosity of soil pore systems and the high affinity of soil constituents to strongly adsorb phosphates compared to diffusion in aqueous solution by a factor of 10^3 to 10^6 (Barber 1995). As a consequence of the much slower diffusion from the bulk soil solution into the rhizosphere, soil solution phosphate is much faster taken up by roots than it can be resupplied by diffusion into the rhizosphere; this results in depletion zones around the roots (Smith et al. 2003; Nussaume et al. 2011). Additionally to the physical processes of mass flow and diffusion, there are also chemical and plant physiological interactions that account for root-induced depletion and replenishment of P in the rhizosphere soil solution. Major plant activities to increase the amount of available P are changes of the rhizosphere pH by roots. Such changes mostly arise from plant release of H^+ and OH^-/HCO_3^- to counterbalance net excess of anions or cations taken up by the roots. With respect to this, occurrence and uptake of plant available nitrogen species is decisive, because not only nitrogen is the ionic nutrient with the highest uptake rates, but it also occurs as both, cation, NH_4^+ , and anion, NO_3^- . Therefore, plants which take up mainly nitrate have a net release of anions such as OH^- resulting in an alkalization of the rhizosphere, whereas plants taking up ammonium show a net release of cations like H^+ , thereby acidifying the rhizosphere (Hinsinger 2001). The exudation of organic compounds such as e.g. citrate also contributes to an acidification of the rhizosphere solution, although indirectly. Compounds like citrate, malate, oxalate, etc. are exuded as anions and not as acids. Therefore, their release is coupled with the release of protons to

compensate for the net efflux of anions. After all, the contribution of exuded organic anions to the changes in rhizosphere pH is small compared to the effects of the uptake of major nutrients, as could be shown especially in the case of maize (Hinsinger 2001). As organic compounds exuded by roots are an important source of energy for rhizosphere microbes (bacteria, protozoa, fungi), the respiration of these compounds results in an acidification of the rhizosphere, as CO₂ and hence carbonic acid (CO₂ + H₂O ⇌ H⁺ + HCO₃⁻) is accumulated in the soil. In soils with low permeability for gases and in alkaline to neutral soils microbial and root respiration significantly contribute to rhizosphere acidification (Hinsinger 2001). Additionally plants are also capable of active, *i.e.* ATP-driven H⁺ release in case of P deficiency, although sites of proton exudation are restricted to areas behind the root tips only (Hinsinger 2001; Marschner and Marschner 2012). Because of the relevant portion of phosphorus that is bound to soil colloids, the process of ion exchange, which is the desorption of nutrient ions from soil particles into the soil solution in exchange for other ions, is of great importance for plants. Main exchange ions delivered by plants are H⁺ ions that are pumped out of the cell by proton ATPases, and HCO₃⁻ coming from root respiration CO₂. The acidification of the rhizosphere increases the solubility of phosphate in close proximity to the roots (Bresinsky et al. 2008). Also the dissolution of phosphate rocks such as apatite-like Ca phosphates is enhanced as the pH is decreased. Together with that, the availability of Ca phosphates in the rhizosphere solution is increased (Hinsinger 2001). Moreover the rhizosphere pH has an influence on the proton electrochemical gradient as the driving force for proton-coupled solute transport as in the case of phosphate uptake (Marschner and Marschner 2012).

1.1.3. Apoplastic vs. symplastic P uptake

For solutes such as phosphate there are two ways of uptake into the root tissue: either *apoplastic* uptake or *symplastic* uptake.

The apoplastic uptake into the root tissue is the movement of phosphate from the external solution into the water-filled space between the root cells. The space between the root cells is a cell wall continuum that consists of cellulose, cross-linking glycans, and glycoproteins, all embedded in a pectin matrix. This highly porous cell wall continuum is the so-called *apoplast* (or *apoplasm*). The movement into the apoplast is a non-metabolic, passive (*i.e.* a non-ATP-consuming) process, driven by diffusion or mass flow. Eventually the Casparian strip of the endodermis confines the direct apoplastic uptake from the external solution and therefore

phosphate has to pass cell membranes for further transport into root tissues. The Casparian strip is the boundary of the root cortex and a barrier of endodermal cell wall parts made of (hydrophobic) suberin and lignin that prevents water and solutes from flowing through the cell wall pores (Bresinsky et al. 2008; Purves et al. 2006; Smith et al. 2003; Marschner and Marschner 2012). However, the endodermis is not a perfect barrier to apoplastic transport. Besides special passage cells in some plant species, there are at least two sites along the root axis where water and solutes can enter the stele apoplastically. The first site is the root apex where the Casparian strip has not fully developed yet; the second sites are basal root zones where lateral roots emerge from the pericycle and thereby disrupt the structural continuity of the endodermis transiently (Marschner and Marschner 2012).

The symplastic uptake is the uptake of solutes into the interconnected cytoplasm of root cells across the plasma membrane and may occur either at the rhizodermis and the root hairs or within the apoplast (Bresinsky et al. 2008; Marschner and Marschner 2012). The continuum of cytoplasm of different cells that are connected by plasmodesmata is the co-called *symplast* (or *symplasm*). Plasmodesmata are junctions of the cell membranes of adjacent cells through their cell walls, which can be closed and opened thereby enabling cells to communicate via transcriptional factors and microRNAs, and to regulate *e.g.* ion fluxes (Marschner and Marschner 2012). Thus symplastic transport means that the transported solute does not pass a cell membrane and therefore stays within the cell plasma of different cells across which it is transported. The plasma membrane is the main site of selectivity in the uptake of solutes as the phospholipid bilayer of the plasma membrane prevents the indiscriminate movement of solutes from the apoplast into the cytoplasm and from the cytoplasm into the apoplast. Symplastic uptake of phosphate is facilitated by integral membrane proteins (Bresinsky et al. 2008; Purves et al. 2006; Smith et al. 2003; Marschner and Marschner 2012).

1.1.4. Transmembrane transport in plants

As already mentioned, water and solute flow is blocked by the Casparian strip on the way to the stele; instead of passive (*i.e.* non-ATP-consuming) flow specific, ATP-consuming transporters in the membranes of cortical and endodermal cells select which nutrients are to be taken up into the symplast. The uptake process of phosphate through the membrane of root cells follows an electrochemical gradient that is maintained by ATPases which function as proton pumps: since protons are concentrated outside of the cell membrane by ATP-

driven proton pumps, an H⁺-phosphate symport can occur against a steep concentration gradient between the exterior solution and the cell plasma (Bresinsky et al. 2008). These concentration differences can be quantified as 5-20 mmol L⁻¹ inorganic phosphate within the cell plasma against usually less than 10 μmol L⁻¹ of plant available phosphate in the soil solution (Raghothama 1999; Nussaume et al. 2011). Phosphate within the cell is not reduced but is to be found as inorganic phosphate in ester bonds or in anhydride bonds (*e.g.* nucleic acids, phospholipids, ...) or in phytic acid, also known as inositol hexakisphosphate, which serves as a storage molecule especially for phosphate (Bresinsky et al. 2008).

1.1.4.1. Michaelis-Menten kinetics

Although the specific mechanisms and transporters involved in phosphate uptake were yet unknown, Emanuel Epstein postulated an analogy between solute uptake by plant cells and enzyme-driven catalytic reactions due to the mechanistic similarity of the nutrient uptake and enzyme reactions (Epstein and Hagen 1952; Epstein 1953). He recognized that plants with arrested metabolism (*e.g.* experiments at 4°C) fail to accumulate nutrients even along a concentration gradient. He also recognized that the uptake against a concentration gradient obviously requires metabolic activity, and that plants accumulate potassium against a concentration gradient despite high sodium (sodium being the competing ion to potassium, as both have the same charges) concentrations in the external solution. Therefore, he hypothesized “that the absorption of inorganic ions involves their combination with binding compounds” (Epstein and Hagen 1952). Evidence could be established that there are several different reactive sites involved in the binding of alkali cations in the case of barley, and that these reactive sites show different affinities for various cations. As ions are evidently present in their free ionic form in the cytoplasm, Epstein concluded that the binding of the nutrients must be transient. He assumed that the ions form a compound with the binding molecule at the outside of the membrane, that the ions are traversed by these molecules and released into the cytoplasm afterwards, following a breakdown of the transient compound. Epstein saw an analogy between this process of ion uptake and the kinetics of enzyme-substrate catalytic reactions (Epstein 1953). Therefore he introduced and adopted the Michaelis-Menten model, which had originally been developed for enzyme-substrate reactions, as a plant nutrient model (Marschner and Marschner 2012). The Michaelis-Menten model was introduced in 1913 by Leonor Michaelis and Maud Menten (Michaelis and Menten 1913) to account for the kinetics of enzyme-catalyzed reactions and describes *inter alia* the affinity of

an enzyme for a certain substrate (Michaelis and Menten 1913; Eckert et al. 2002; Purves et al. 2006). According to that adoption transport proteins across the membranes were supposed to function like enzymes, while ions in external solutions were considered to function as substrates to be catalyzed, *i.e.* transported from one side of the membrane to the other. The adoption of the Michaelis-Menten model appears as follows:

Equation (1) displays the original Michaelis-Menten equation, where V is the reaction rate at the substrate concentration $[S]$, V_{max} is the maximum reaction rate at substrate saturation and K_m is the Michaelis-Menten constant (*i.e.* the concentration of the substrate at which $V=V_{max}/2$) that indicates the affinity of the enzyme for its substrate:

$$(1) \quad V = \frac{V_{max} [S]}{K_m + [S]}$$

According to the need of an adaption of the original equation, equation (2) was obtained, where I is the ion uptake rate at the ion concentration C in the external solution, I_{max} is the ion uptake rate at saturation in the external solution:

$$(2) \quad I = \frac{I_{max} C}{K_m + C}$$

1.1.4.2. Phosphorus efflux

The fact that plants not only take up nutrient ions but also release them into the external medium was already discussed and investigated in the 19th century. First experimental work was inspired by Augustin Pyramus de Candolle's crop rotation theory (Merrill 1915) which was based on the assumed excretion of harmful substances by roots. De Candolle claimed that crop plants that succeeded related plants on the field would not prosper due to toxic excretions of the earlier crop. Following this theory, many experiments were conducted delivering contradictious results. First evidence for de Candolle's theory was delivered by M. Macaire in 1832 (Merrill 1915) who took plants from soil and placed them onto vessels filled with rain water. Due to changes in colour and odour he concluded that certain substances had been excreted by the plant roots. Although many arguments were made against de Candolle's and Macaire's case, further investigations on the subject were conducted. A.

Gyde (Merrill 1915) grew plants on soil and put them onto distilled water for 3-17 days in 1847. Then he evaporated the water and found organic and inorganic residues. Plants that were grown on solutions made from those residues did not show any disturbances of growth. W. Knop (Merrill 1915) conducted a series of experiments between 1860 and 1864 to study the character and the amount of root excretions from plant roots into distilled water. With respect to inorganic excretions his analyzes indicated the release of potassium, calcium and phosphoric acid into the water. F. Czapek (Merrill 1915) analyzed the exact chemical nature of the excreted substances (around 1900) and thereby identified *i.a.* K, Ca, HCl, H₂SO₄ and H₃PO₄. However, all these experiments did not allow definite conclusions since experimental work and results were solely based on the use of electrolytic or qualitative chemical techniques. Hence, accurate determinations of low concentrations and of ion fluxes in a direction opposite to that of net ion flow was not possible. In the 1940s and early 1950s data from studies concerning root ion losses into growth media and the reduction in the nutrient content of plant tops delivered evidence for the assumption that root ion losses may play an essential role in the overall nutrient economy of a plant (Emmert 1959). Since the late 1940s the development of radioisotope methods made possible the exact measurement of very low concentrations and the movements of ions. Emmert (1959) showed clearly that ³²P applied on the leaves of *Phaseolus vulgaris* L. passed through the roots into the external solutions. He also showed that the amount of the radioisotope found in the exterior solution depends on the phosphorus concentration of the solution and on its ion content, respectively. Emmert's results corresponded to earlier findings of root ion efflux; nevertheless his data were obtained after foliar application of phosphorus to avoid contaminations and thereby to increase accuracy.

Elliott et al. (1984) investigated the ratios of simultaneous phosphorus influx and efflux. Therefore they grew maize seedlings on nutrient solutions at phosphorus concentrations usually found in soil solutions (about 0.4 and 1.8 μmol L⁻¹). After six days of growth on the nutrient solution, the seedlings were transferred onto ³²P labeled solutions containing 0.2 μmol L⁻¹ phosphorus (specific activity of 8.88×10⁵ cpm μmol⁻¹) and 2.0 μmol L⁻¹ phosphorus (specific activity of 1.22×10⁵ cpm μmol⁻¹), respectively, for 48 hours to label the plants with ³²P. After this period, the roots were rinsed in a phosphorus free solution for ten minutes and then transferred onto ³³P-labeled solutions containing 0.2 μmol L⁻¹ phosphorus (specific activity of 8.88×10⁶ cpm μmol⁻¹) and 2.0 μmol L⁻¹ phosphorus (specific activity of 3.52×10⁶

cpm μmol^{-1}), respectively, for another 10 minutes. For the calculation of the efflux/influx ratios the net depletion of ^{33}P and the appearance of ^{32}P in the nutrient solution were evaluated: The first set of 10 plants labeled on a $0.2 \mu\text{mol L}^{-1}$ phosphorus solution showed a mean efflux rate of $0.24 \pm 0.09 \text{ nmol (g fresh wt root)}^{-1} \text{ min}^{-1}$ and a mean influx rate of $0.27 \pm 0.14 \text{ nmol (g fresh wt root)}^{-1} \text{ min}^{-1}$; the first set of 12 plants labeled on a $2.0 \mu\text{mol L}^{-1}$ phosphorus showed a mean efflux rate of $0.62 \pm 0.35 \text{ nmol (g fresh wt root)}^{-1} \text{ min}^{-1}$ and a mean influx rate of $4.91 \pm 1.33 \text{ nmol (g fresh wt root)}^{-1} \text{ min}^{-1}$; the second set of 12 plants labeled on a $0.2 \mu\text{mol L}^{-1}$ phosphorus showed a mean efflux rate of $0.56 \pm 0.18 \text{ nmol (g fresh wt root)}^{-1} \text{ min}^{-1}$ and a mean influx rate of $0.95 \pm 0.21 \text{ nmol (g fresh wt root)}^{-1} \text{ min}^{-1}$; the second set of 11 plants labeled on a $2.0 \mu\text{mol L}^{-1}$ phosphorus showed a mean efflux rate of $0.52 \pm 0.29 \text{ nmol (g fresh wt root)}^{-1} \text{ min}^{-1}$ and a mean influx rate of $8.44 \pm 1.80 \text{ nmol (g fresh wt root)}^{-1} \text{ min}^{-1}$. As it turned out, the average efflux/influx ratios were 0.68 for the $0.2 \mu\text{mol L}^{-1}$ and 0.08 in the $2.0 \mu\text{mol L}^{-1}$ phosphorus solution. These data and the outcomes of experiments mentioned above clearly show that efflux of phosphorus from roots usually occurs, moreover Elliott showed clearly that “P efflux is a substantial component of net P accumulation at P concentrations normally found in soil solutions” (Elliott et al. 1984).

Another example for ion efflux from roots is provided by Cogliatti et al. (1990), who demonstrate P efflux from wheat seedlings on solution cultures, when they state that P-influx was increased together with a raised external concentration, that I_{max} only changed a little, and that K_m did not change at all (Cogliatti et al. 1990).

Another indication for phosphorus efflux comes from yet a different approach: studies performed to examine the small scale phosphorus distribution in soils and in the rhizosphere using high-resolution chemical imaging. Santner et al. (2012) could not only show depletion zones surrounding root axes, but they also found elevated phosphorus concentrations at several spots along the roots. These hotspots of phosphorus were interpreted as potential sites of phosphorus release from the root into the rhizosphere. As up to this direct observation of P dynamics in the rhizosphere at relevant spatial scales (sub-mm) had been lacking (Santner et al. 2012), the assumption that this might be the first visualization of phosphorus efflux seems justified.

1.1.4.3. P-efflux and the Michaelis-Menten model

Due to the low concentrations of P in soil solutions (about $<1 - 8 \mu\text{mol L}^{-1}$ soil solution (Smith et al. 2003), or $0.2-2 \text{ mg kg}^{-1}$ soil (Blume et al. 2010; Schroeder 1972)) and to findings of

uptake studies conducted also at low concentrations ($<10 \mu\text{mol L}^{-1}$), the term “ C_{min} ” was introduced. Claassen et al. (1974) made use of the Michaelis-Menten model when they evaluated the data they obtained by solution depletion experiments conducted with plants grown on nutrient solutions. In this way, values for the parameters of the model were obtained. Additionally to V_{max} , K_m , and E (efflux), Claassen et al. (1974) also introduced a parameter they called “ C_0 ”, “the ion concentration in solution below which net influx of the ion ceases”(Claassen et al. 1974). When they fit their data of different concentrations of potassium, phosphorus, and nitrogen to the model assuming E to be constant, they found a concentration minimum that was necessary to enable plants to take up the nutrient in question (Fig. 1). But in their discussion they restricted themselves to just stating that C_0 was “a parameter about which little information exists” (Claassen et al. 1974).

So, C_0 or C_{min} describes the external ion concentration at which the ion efflux from the root and the ion influx into the root are equal, therefore the term represents the lowest concentration at which net ion uptake can occur (Marschner and Marschner 2012):

$$(3) \quad I_n = \frac{I_{max} (C_s - C_{min})}{K_m + (C_s - C_{min})}$$

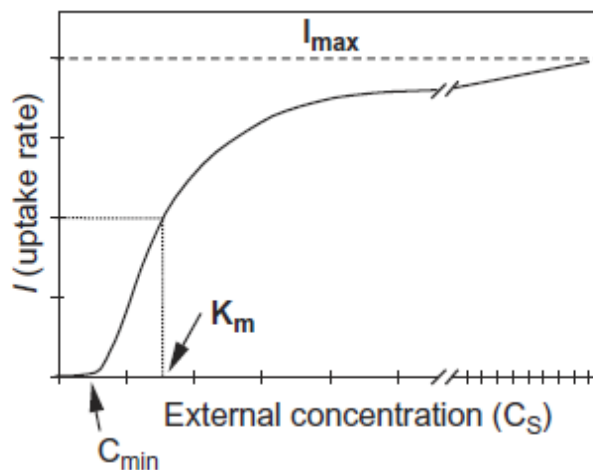


Figure 1: Michaelis-Menten ion uptake curve; reproduced from Marschner and Marschner (2012).

1.1.5. Long distance transport of phosphorus in plants

For the long-distance transport within a vascular plant phosphate has to be translocated across the cell membranes confining the symplast into the apoplast of the stele. The apoplast of the stele is all the dead cells of the xylem which functions as the main transport system up to aerial parts of the plant driven by transpirational pull and root pressure. Another possibility is the transport from the pericycle to the living cells of the phloem (sieve tube elements and companion cells). Phosphate is highly phloem mobile and can thus be transported efficiently by phloem streams (Bresinsky et al. 2008). Phloem transport is different from xylem transport: as xylem streams are always directed upwards following a decreasing water potential, phloem streams (in different vessels) are directed upwards as well as downwards and are independent from transpirationally regulated water potentials. Differences in pressure and thus flowing directions within phloem vessels are brought about by accumulations of sugars and other solutes which osmotically induce the inflow of water and thereby form the starting point of mass flow. Though the processes of ion secretion into the vascular bundles are not clear in all details so far, it is assumed that ions are secreted into the xylem mostly actively and selectively (Bresinsky et al. 2008; Purves et al. 2006; Smith et al. 2003).

1.1.6. Xylem and phloem loading and unloading

Within the living tissue of the stele, phosphate is usually transported symplastically (*i.e.* via plasmodesmata) from the endodermis to the pericycle or to parenchyma cells. (Bresinsky et al. 2008; Purves et al. 2006; Smith et al. 2003; Marschner and Marschner 2012).

Symplastic transport within the stele is confined by the dead cells of the xylem or the living cells of the phloem. The cells of the phloem and the xylem form the vascular bundles, the long-distance transportation system of vascular plants. For the loading of the vascular bundles the activity of membrane transporters is essential. In the case of phosphate the PHT1 protein family is the most important group of transporter proteins in terms of root uptake and redistribution within plant tissues (Nussaume et al. 2011). In the *Arabidopsis thaliana* genome there are genes for nine members of these proteins which are all $\text{H}_2\text{PO}_4^-/\text{H}^+$ symporters: each phosphate molecule is transported into the cell together with a proton against an electrochemical gradient by a trans-membrane protein-transporter. As the concentration of phosphate on the inner side of the membrane is maintained at a level up to eight times higher than on the outside and as the net charge in the cytosol is negative, a

high-affinity and energy-driven transport mechanism is required. The members of the PHT1 protein family fulfill these requirements (Smith et al. 2003). H⁺-ATPases present in the plasma membrane catalyze H⁺ efflux via hydrolysis of ATP, thereby maintaining a proton electrochemical gradient. PHT1 transporters then couple H⁺ influx to movement of phosphate against its electrochemical gradient (Marschner und Marschner 2012).

The unloading from the xylem and the phloem stream can take place all along the entire system of the vascular bundles and phosphate can enter the apoplast or the symplast of the neighboring tissues (Bresinsky et al. 2008). Every time phosphate has to stride through membranes, transport proteins of the PHT1 family play an essential role (Smith et al. 2003). Due to its high mobility within the plant, apparently phosphate can be distributed quickly throughout all tissues.

1.2. Objectives

As we know that efflux of phosphate from roots into the rhizosphere occurs and phosphorus hotspots in the rhizosphere can be shown, we were interested in establishing an efflux-related explanation of these phosphorus hotspots. So the aims of this master project were:

1. to investigate the source of possible P hotspots at the root tips that were observed in Santner et al. (2012) using DGT-LA-ICP-MS-based chemical imaging. Potential sources are P solubilizations from the soil as well as P efflux from plant roots;
2. to make sure that the possibly observed phosphorus efflux does not occur due to root injuries;
3. the relative quantification of root phosphorus efflux at different root segments along the root axis using autoradiography.

2. Material and Methods

2.1. Growth media

For both experimental setups, *i.e.* the experiments using DGT-LA-ICP-MS-based chemical imaging and those using autoradiography, maize plants were grown in rhizotrons. Rhizotrons are plant growth boxes made of Plexiglas with a removable plate on the front; they are about 40 cm long, 10 cm wide, and 1.5 cm deep. As rhizotrons are set up in a sloping manner plants are forced to develop their roots along the inclined removable front plate. After sufficient root growth the front plate can be removed leaving the roots ready for sampling.

In both cases plants were grown on soil, for the ^{33}P efflux experiments additional maize plants were grown on agarose gel in rhizotrons.

2.1.1. Soil

For the ^{31}P experiments as well as for the ^{33}P efflux experiments two low P soils, with and without P fertilization, respectively, were used

“*Forchtenstein/Grünland*”: This is an acidic soil from a meadow in Forchtenstein in the province of Burgenland, Austria.

“*Santomera*”: This is an alkaline soil from the municipality of Santomera in the region of Murcia, Spain.

Soil	pH (CaCl ₂)	P _{CCAL} unfertilized mg kg ⁻¹	P _{CCAL} fertilized mg kg ⁻¹
Forchtenstein/Grünland	4.75	12.4	28.9
Santomera	7.56	39.1	49.3

Table 1 displays the soil property data that were measured before actual experiments were conducted.

Both soils were fertilized with a balanced variety of nutrients¹ except phosphorus. Additionally two treatments with phosphate fertilization were prepared. Thereby four different treatments were obtained in total.

¹ For details on nutrient amounts see appendix.

The soils were sieved to >2 mm. For soil fertilization, 181.1 mg of NH_4NO_3 , 124.5 mg KCl, 134.3 mg MgCl_2 , 33.9 mg ZNSO_4 , and, for the P-fertilized soils, 45.9 mg KH_2PO_4 were added to 1 kg of soil. Therefore, nutrient stock solutions were prepared. Adapted amounts of these stock solutions were poured onto subsamples of readily weighed soil treatments and dried in an oven at 50°C for about 24 hours. Afterwards, the fertilized subsamples were homogenized and mixed back into the larger soil samples (=6 kg each) of soil. The soils of all four treatments were moistened with a stirrup pump filled with Millipore water and were intensively mixed, always with regard on avoiding soil clumping. After moistening the soils were put into open plastic bags and transferred to an incubator for 6-7 days at 20°C where they were allowed to equilibrate.

For both types of experiments the fertilized, moistened, and equilibrated soils were filled layer upon layer into rhizotrons resulting in soil column dimensions within the rhizotron of 100 x 15 x 363-382 mm (WxDxH). Each layer was gently compacted with a tightly fitting plastic strip, reaching net soil weights of 648-757 g per rhizotron and bulk soil densities of 1.15-1.24 g cm^{-3} .² After filling, the open-top surfaces of the rhizotrons were covered with disposable gloves to avoid soil drying. The rhizotrons were put into the incubator at 20°C until watering and planting of the germinated seedlings.

2.1.2. Agarose gel

While for the preliminary experiments a set of rhizotrons with inner dimensions of 149 x 20 x 400 mm (WxDxH) was filled with Gelrite (of which only one could be used for sampling), for the main efflux experiments an additional set of rhizotrons with the same dimensions, filled with an plant growth agarose gel layer with a thickness of about 10 mm, was prepared. Gelrite was originally chosen because of its higher strength, but was then exchanged for plant growth agarose because of adopting a whole method based on this gel. The agarose gel was prepared according to a protocol³ the author got from Dr. Gerlinde Wiesenberger from the Department of Applied Genetics and Cell Biology at the University of Natural Resources and Life Sciences, Vienna. For the preparation of the agarose gel a modified Murashige-Skoog nutrient mixture was used. For each rhizotron 600 mL –resulting in 10 mm thick agarose layer – of agarose medium were prepared by following procedure:

² For details on individual rhizotron soil densities see appendix.

³ For details on this protocol see appendix.

600 mL of Millipore water was transferred into an autoclavable bottle which was put onto a magnetic stirrer; to each bottle an autoclaved stirring bar was added; 2.64 g (4.4 g L⁻¹) of nutrient salt were added; after its dissolution 0.36 g (0.6 g L⁻¹) MES were added and the pH was adjusted to 5.7 – 5.8 by adding NaOH in small drops; finally 4.8 g (8 g L⁻¹) of solid agar were added and stirred until all solids were dissolved. After the mixing procedure the bottles and their contents were autoclaved at 140°C for at least 30 minutes. The autoclaved liquid agarose mixtures were filled into the disinfected rhizotrons (the rhizotrons were washed in a bath containing 7.2 g sodium hypochlorite L⁻¹).

2.2. Diffusive gradients in thin films technique – DGT

The diffusive gradients in thin films technique (DGT) was introduced by Davison and Zhang (1994). Originally it was developed to measure labile species quantitatively in marine and freshwater systems (Davison and Zhang 1995). Today it is also successfully applied to sediments and soils. It can be used for different purposes and methods such as *in situ* measurements, monitoring, speciation, investigations of fluxes and kinetics, and studies on bioavailability (Zhang, 2003). Moreover, it has also been used for chemical imaging of different analytes, *e.g.* phosphorus (Santner 2012). To measure a dissolved species, the DGT device needs to comprise a selective binding agent. Trace metals such as *i.a.* Al³⁺, Cd²⁺, Co²⁺, Cs²⁺, Cu²⁺, Fe²⁺, Mn²⁺, Ni²⁺, Pb²⁺, Zn²⁺, and anionic species like PO₄³⁻ can be sampled (Zhang 2003). In the case of this thesis it made also possible the investigation of root efflux of phosphate into the rhizosphere.

2.2.1. Function

DGT measurements are based on diffusion. As diffusive fluxes occur along a concentration gradient towards a sink, the analyte of interest diffuses into the DGT sampler which serves as a zero-sink. In DGT samplers, a diffusive gradient is established by the combination of two different gel layers:

A hydrogel layer serves as a well-defined diffusion layer. For the hydrogel, a water content as high as 95 % is possible and results in almost unrestricted diffusion of all chemical species with a molecular size smaller than the pores of the hydrogel (Zhang and Davison 1999; Davison and Zhang 1995). The ideal DGT hydrogel has a functional pore size from 2 to 5 nm (the diameters of most hydrated cations range between 0.2 to 0.3 nm). But diffusion coefficients of ions within hydrogels are not the same as in pure water due to the tortuosity

and permeability of the gel that lower the rate of diffusion. Therefore, diffusion coefficients of different analytes at different temperatures have been measured and set up in tables (Zhang 2003). Usually the hydrogel layer has a thickness of 0.8 mm.

The second layer is the binding layer. Generally, it consists of a polyacrylamide hydrogel with a binding agent that is selective for the analyte in question. Ions that pass the diffusion layer are rapidly adsorbed and immobilized in this binding gel. (Zhang 2003; Zhang and Davison 1995). According to the analyte, there are various binding layers. In case of phosphorus an iron oxide gel was introduced by Zhang et al. (1998). As long as the binding capacity is not exceeded, the concentration of the analyte at the surface of the binding layer is maintained at zero and a concentration gradient in the hydrogel layer is maintained (Zhang 2003).

2.2.2. DGT gel preparation

All experiments conducted in this master project used ferrihydrite DGT for phosphate sampling. Those DGT gels were prepared as follows:

Casting of polyacrylamide diffusive gels: First all casting devices, *i.e.* glass plates and spacers, were acid washed (in a 5% HNO₃ solution), rinsed properly with deionised water with an electrical resistance of 14.1 MΩ cm⁻¹ (in the following referred to as Millipore or HQ water) and air-dried. Then two glass plates were clipped together with a spacer in-between, for easier pipetting the glass plates were offset for about a millimeter on the top side without spacer.

For the preparation of DGT gels 10 mL of gel solution (containing 15% acrylamide and 0.3% DGT cross linker) and 70 µL of a 10% ammonium persulphate solution followed by 25 µL of a 99% tetramethylethylenediamine (TEMED) solution were mixed.

About 4 mL of the mixture were pipetted between the glass plates for a gel strip with a thickness of 0.8 mm and about 2 mL for a gel strip with a thickness of 0.4 mm.

The assemblies were put into an oven at 42°C for one hour. Afterwards the assemblies were opened, gels were removed and washed. Therefore, the gels were put into one liter HQ water and then transferred into another liter of HQ water for hydration. A few hours later the water was changed again; the change was repeated another two times. In total the water was changed four times during 24 hours of hydration. The gels were stored in a 0.01 mol L⁻¹ NaNO₃ solution.

Precipitation of ferrihydrite in polyacrylamide diffusive gels: 2.7 g FeCl₃(H₂O)₆ were dissolved in about 40 mL Millipore water in a clean container. Up to three diffusive gel strips were put

into this solution; the container was filled up to 100 g net weight (including the gels) gravimetrically. The final concentration of FeCl_3 in the solution was 0.1 mol L^{-1} . Gels were allowed to equilibrate in the solution on a horizontal shaker for at least two hours.

For ferrihydrite precipitation the gels were transferred into 100 mL MES buffer (containing 0.05 mol L^{-1} MES, pH adjusted to 6.7) and stirred immediately after transfer for a few minutes in order to avoid heterogeneous distribution of ferrihydrite on the gel. Then the gels were allowed to soak for about 30 minutes.

After precipitation the gels were washed in 1L HQ water, after a few minutes the water was changed, after about two hours the water was changed again; changing and soaking were repeated for another 2-3 times to remove excess reagents.

After washing the ferrihydrite gels were transferred into 0.01 mol L^{-1} NaCl solution. After a 24 hours' storage the gels were ready for use for at least one month.

2.3. Colorimetric determination of P

Throughout this work, colorimetric analysis for determining phosphorus concentrations in DGT eluates and in plant root digests was conducted using a Hitachi U-2000 Spectrophotometer.

Therefore, the molybdenum blue batch method as described in (Zhang 2003) was used. There are two slightly different variations of this method: while one (1) is the analysis for samples containing 0.25 mol L^{-1} H_2SO_4 (e.g. DGT eluates), the other one (2) is for samples containing no sulphuric acid.

The following stock solutions are needed:

- A. H_2SO_4 : 2.5 mol L^{-1} (247 g dissolved in about 500 mL water, filled up to 1000 mL when cooled)
- B. Ammonium heptamolybdate: 0.03 mol L^{-1} (20 g dissolved in 500 mL)
- C. Potassium antimonyl tartrate: 0.004 mol L^{-1} (0.28 g dissolved in 100 mL)
- D. Ascorbic acid: 0.1 mol L^{-1} (1.76 g dissolved in 100 mL)

From these stocks, the following mixed reagents were prepared according to the sample acid content in following way:

(1) for samples containing 0.25 mol L^{-1} sulphuric acid:

- 10 mL water + 3 mL B + 1 mL C
- for the staining, 1.4 mL of the mixed reagent are added to 10 mL of sample followed by 0.6 mL of D.

(2) for samples containing no sulphuric acid:

- 10 mL of A + 3 mL of B + 1 mL of C + 6 mL of D
- for the staining, 2 mL of the mixed reagent are added to 10 mL of sample

After addition of reactants to the samples, the development of color was allowed for about 15 to 20 minutes. The samples were measured immediately afterwards.

2.4. ³¹P-efflux experiments

After the seven day equilibration and incubation period, the rhizotrons were opened. A polytetrafluoroethylene (“Teflon”) foil was applied on the open side of the rhizotrons for separating the watered soil and the roots on the one hand and the rhizotron cover on the other hand. For setting the soil water content to about 30% of the maximum water content, the rhizotrons were watered through the 14 holes on the bottom side of the device with adequate amounts of water.⁴

Subsequently the *Zea mays* seedlings were planted into the rhizotrons: Therefore “NK Falkone”-cultivar seeds⁵ (were sown onto wet paper towels in Petri dishes and germinated under warm conditions (about 25°C). Three days after germination the seedlings were transferred to the rhizotrons. For planting, holes with 2 cm of depth were formed in the middle of soil surface in the rhizotrons, the seedlings were put into these holes and covered with soil, slightly pressed into the soil and finally watered with 2 mL Millipore water. After planting, the rhizotrons were put under plant cultivation lamps (lighting 16 hours per day: 100-150 $\mu\text{mol photons m}^{-2} \text{s}^{-1}$; temperature: 24-26°C) and put up in an inclined manner (with an angle of about 45° between floor and rhizotrons). After seven days of growth in the rhizotrons (ten days after germination) four rhizotrons with suitable roots were chosen for DGT sampling.

⁴ For the watering protocol see appendix.

⁵ “NK Falkone” is the most popular maize cultivar in Austria for the production of grain maize; it is produced by Saatbau Linz OÖ Landessaatbaugenossenschaft GenmbH., by courtesy of which we received seeds for our experiments.

2.4.1. DGT sampling setup

For sampling, the selected rhizotrons were put onto a stage assembled with retort stands in a horizontal way. To each rhizotron 14 hoses connected with a water container were applied on the downside of the devices by sealed screw tops. The containers were filled with water and raised above the rhizotrons. By this, water flowed from the container to the rhizotrons and saturated the soil therein within a few hours. When water saturation of the soils in the rhizotrons was reached, the cover plates and the polytetrafluoroethylene (PTFE) foils were removed. Meanwhile, DGT strips were cut according to the format and size of the root sector chosen to be sampled. The readily cut DGT strips were put onto the plates of the rhizotron at the right spot (Fig. 2a), covered with a polyethersulfon (PES) membrane (0.2 μm pore size, manufactured by Pall) and fixed with a waterproof adhesive tape. For the sampling

the cover plates on which the DGTs were applied, were put back on the rhizotrons carefully and fixed onto them with clamps. For the next 24 hours DGT gels were allowed to take up phosphorus from the watered soil by diffusion. Afterwards the cover plates were removed, the membranes were rinsed with Millipore water, and cut from the plate so that the DGTs underneath could be removed. After removal, the DGT gels were put onto a suitable structure membrane (the orientation of each DGT was written

down), then they were put into plastic bags, the plastic bags were cut along the membranes thereby obtaining a protective foil layer on the DGT. The

DGTs on the structure membranes were assembled on a blotting paper and dried in a vacuum device overnight (Fig. 3). The DGTs were now fixed and – after gluing onto glass plates (Fig. 4) – ready for laser ablation ICP-MS (Fig. 2b).

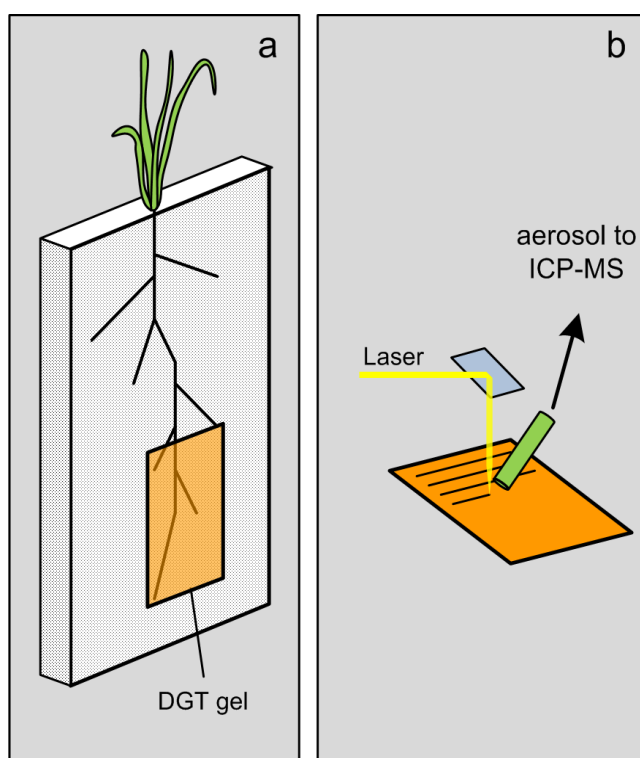


Figure 2: The fundamental scheme of the DGT sampling procedures and the LA-ICP-MS measurement. (a) First the DGT strips are applied onto the chosen rhizotron/root surface area, and then (b) the DGT gels are ablated and measured line after line (figure by courtesy of Jakob Santner).

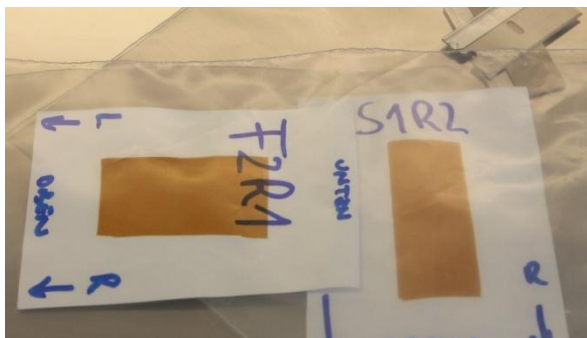


Figure 3: Dried DGTs on structure membrane ready to be glued onto glass plates.



Figure 4: Dried DGTs on cut-out structure membrane glued onto glass plates – ready for laser ablation.

2.4.2. Preparation of DGT standards for laser ablation ICP-MS

For the preparation of DGT standards necessary for the calibration of the DGT samples shown above, DGT samplers were assembled and allowed to take up phosphorus by diffusion from different solutions and within different periods of time.

2.4.2.1. Assembly of DGT samplers

The DGT samplers were assembled in the following way (Fig. 5): a ferrihydrite gel disc with a diameter of 2.5 cm and a thickness of 0.4 mm was put onto a piston, followed by a PES membrane disc (0.2 μm pore size; not shown in Fig. 5) to prevent the two gel discs from sticking together, then a pure diffusive gel disc with a diameter of 2.5 cm and a thickness of 0.8 mm was added followed by a protective, outer nitrocellulose membrane filter (0.45 μm pore size, manufactured by Whatman). Eventually a cap was put onto the piston to close the sampling the device. After the assembly, the samplers were bagged and stored in the refrigerator for a few days.

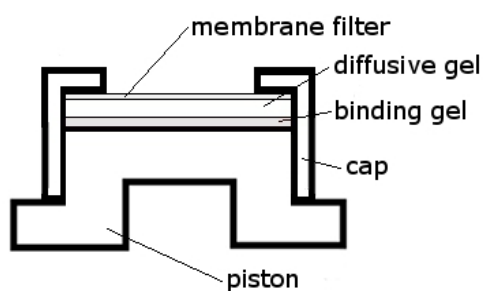


Figure 5: Left: cross-section of a DGT sampler showing the different layers within the device. An additional layer, a membrane disc, was inserted between the binding ferrihydrite gel and the diffusive gel (Santner 2014). Right: depiction of an assembled DGT sampler as it is deployed for diffusion experiments (picture taken by the author).

2.4.2.2. Loading of the DGT standards

Before the deployment of the samplers three different phosphorus solutions were prepared. For each 3 L solution different amounts of phosphorus stock solution containing 1000 mg $\text{PO}_4^{3-} \text{L}^{-1}$ (= 326 mg P L^{-1}) were added: to the first 0.144 mL were added; to the second 0.575 mL and to the third 1.15 mL were added. Additions of these amounts of stock solution result in 15.7 $\mu\text{g P L}^{-1}$ in the first case, 62.5 $\mu\text{g P L}^{-1}$ in the second case, and 125 $\mu\text{g P L}^{-1}$ in the third case (Tab. 2). To all three solutions 30 mL of a 1 mol L^{-1} NaCl solution were added (resulting in 0.01 mol L^{-1} NaCl) as a background electrolyte. The solutions were allowed to equilibrate while being stirred in closed containers already containing mountings for the DGT samplers for seven days.

After equilibration, the solutions were exchanged with freshly prepared, pH adjusted solutions (pH 5.8). Then the DGT samplers were installed on the mountings: in each the first and the second solution 4 samplers were immersed, in the third six samplers were immersed. In total, seven different standards with two repetitions were prepared. Additionally three blanks were put aside (they were not immersed in any solution but stored in the refrigerator). During the deployment, the solutions were well stirred to minimize the thickness of the diffusive boundary layer surrounding the samplers. Before and after each treatment samples of 5 mL of the immersion solutions were collected. After the removal from the solutions, all samplers were taken apart, the ferrihydrite gels were weighed, cut into halves and each half weighed separately. One half of every disc was put into an Eppendorf vial, while the other half was put onto a foil and packed into a plastic bag. The bagged halves were put onto structure membranes and dried in a vacuum device overnight. After drying, the halves were cut again, resulting in quarters of the whole discs. One quarter of one standard disc of each treatment and one quarter of each blank was glued onto a glass plate and used for calibration in the LA-ICP-MS analysis. The other halves of the DGT standard discs in the Eppendorf vials were each eluted in 500 μL of 0.25 mol L^{-1} H_2SO_4 . The phosphate concentrations of these eluates were then determined by colorimetric analysis using the molybdenum blue batch method (see 2.3). Therefore, the eluates were diluted with 0.25 mol L^{-1} H_2SO_4 and colored according to preparation method (1). A calibration series was prepared from a 1000 mg L^{-1} PO_4 photometer standard for phosphorus concentrations of 10, 25, 50, 100, 250, and 500 $\mu\text{g L}^{-1}$.

The calculation of the phosphorus surface concentration of the standards follows these two equations:

$$(4) \quad C_{surface} = \frac{M}{A}$$

where M is the absolute amount of phosphorus on the gel, and A is the exposure area of the gel ($A = 3.14 \text{ cm}^2$).

$$(5) \quad M = \frac{C_e (V_{acid} + V_{gel})}{f_e}$$

where C_e is the concentration of P in the gel eluate (in $\mu\text{g L}^{-1}$), V_{acid} is the volume of 0.25M H_2SO_4 added to the Fe-oxide gel, V_{gel} is the volume of the Fe-oxide gel, typically 0.16 ml. f_e is the elution factor for P, which is 1 in this case.

Standard	Nominal P loading $\mu\text{g cm}^{-2}$	Time h	Deployment solution P concentration $\mu\text{g L}^{-1}$	Calculated P-stock mL L^{-1}
1	0.01	3	15.6	0.144
2	0.02	6	15.6	0.144
3	0.04	3	62.5	0.575
4	0.08	6	62.5	0.575
5	0.12	4.5	125	1.149
6	0.16	6	125	1.149
7	0.20	7.5	125	1.149

Table 2 shows the preparation features of the calibration standards for the laser ablation ICP-MS.



Figure 6: Assembled DGT standards ready for Laser ablation ICP-MS.

2.4.3. Laser ablation ICP-MS

As described in Santner et al. (2012), high-resolution two-dimensional chemical imaging of solutes in the rhizosphere can be achieved by sampling using diffusive gradients in thin films technique (DGT) coupled with laser-ablation inductively coupled mass spectrometry (LA-ICP-MS). P in the soil solution is absorbed by the DGT gel and bound to the ferrihydrite causing a diffusion flux from the soil surface to the DGT gel. P that is adsorbed by the gel is derived from P that desorbs from soil solid constituents into the soil solution. During the sampling period, usually 24 hours, the P flux to the DGT gel decreases. As P concentrations across the sampling area vary, P fluxes towards the gel are different and therefore result in an inhomogeneous areal P loading on the DGT gel. Because this method achieves the direct observation of P dynamics in the rhizosphere at sub-mm scale, it was chosen for the establishment of proof for phosphorus hotspots in the rhizosphere of *Zea mays*.

The DGT strips from the hotspot experiments as well as the calibration standards, both glued onto glass plates, were analyzed by LA-ICP-MS (Fig. 2b) using a Perkin Elmer NexION 300D ICP-MS connected to a New Wave UP-193-FX laser ablation system.

The sweep time was 0.11 seconds with 4 sweeps per reading which results in a dwell time (analysis time for recording one ICP-MS reading) of 0.44 seconds. The diameter of the ablating laser spot was set to 150 μm , laser energy was adjusted to 40%. Line length was 20,000 μm with an offset between the lines of 350 μm and a total line count of 115 lines. Therefore, the total scan distance equals 230 cm. Laser speed was set to 300 $\mu\text{m s}^{-1}$ with a washout delay of 10 seconds and a reposition safety time of 3 seconds after each line, summing up to 79.7 seconds for each line. In these 79.7 seconds the ICP-MS recorded 181.1 readings.

These settings result in an x-resolution of 132 μm and a y-resolution of 350 μm . The scanned surface area comprises about 8 cm^2 .

After following the starting, rinsing, and tuning procedures for both, the ablation system and the mass spectrometer, the ablation pattern was set manually and then the measurement was started. In total four DGT gel samples as deployed in the sampling setup were measured in four days; before each measurement DGT blanks and DGT calibration standards were measured.

2.5. ³³P-efflux experiments

The second and more important experimental approach for answering the research questions was a series of phosphorus efflux experiments using ³³P, a radioisotope of phosphorus, to label the P in plant shoots combined with 2D DGT sampling and autoradiography of plant roots and DGT rhizosphere samples. Quantification of effluxed phosphorus was sought to be achieved using a combination of plant digestion, scintillation counting, colorimetric determination of phosphorus, and autoradiography.

2.5.1. Preliminary experiments

Just as for the phosphorus hotspot experiments, rhizotrons were filled with soil. Additionally a series of rhizotrons filled with agarose gel was used.⁶ But before the actual DGT sampling could be carried out, several preliminary experiments had to be done.

2.5.1.1. Radioactive plant labeling

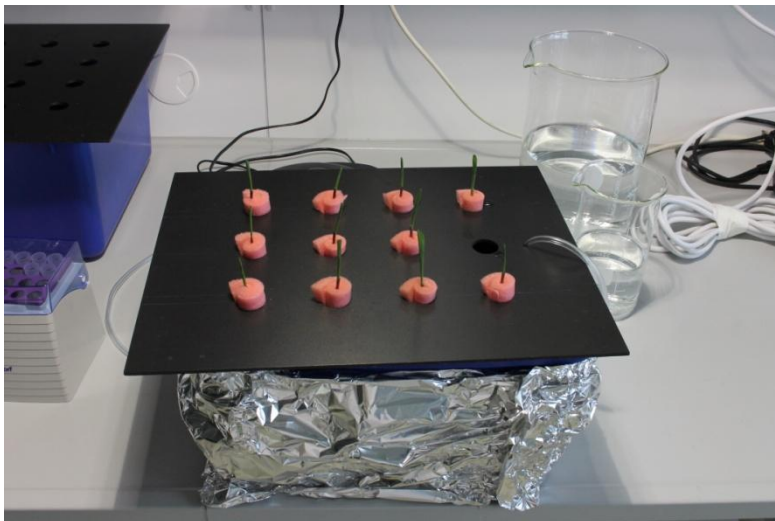


Figure 7 (left): The readily planted and operative hydroponic container.



Figure 8 (right): Close-up of a seedling on the container wrapped in a strip of a cleaning sponge.

Because there was no detailed protocol for introducing ³³P into plant shoots, a procedure had to be developed. For this reason a few preliminary experiments with hydroponics were conducted. Maize seeds were germinated in a rolled-up sterile paper towel wrapped in plastic foil to prevent drying of the paper; then this longish “germ-wrap” was put into a beaker half-filled with Millipore water. Two days later the plants were transferred to a

⁶ See appendix for the list of rhizotrons.

beaker half-filled with a nutrient solution⁷ without phosphorus. Another two days later the seedlings were put onto a hydroponic container filled with 12 L nutrient solution (the same solution as used for germinating) (Fig. 7 and 8). The solution was aerated through a hose by a pump usually used for fish tanks. The container was packed in aluminum foil to prevent the growth of algae. After one day of growth on the 12 L container, six plants were transferred onto 500 mL containers, each aerated by one hose. The plants left on the large hydroponic container were kept as a reserve. While three vessels contained a nutrient solution with phosphorus (+P, 13.6 mg L⁻¹ KH₂PO₄), the other three did not contain any phosphorus (-P). On these plants three different methods of labeling with radioactive ³³P were tested. For each method one +P and one -P plant were used.

1) A leave tip was removed with a clean razor blade cut and then immersed into 1 mL of a radiolabeled phosphate solution (³³P, about 30 μCi) in an Eppendorf vial.

2) The coleoptiles of two plants were punctured with a tip of a pair of tweezers and then an acidic (pH 2) droplet (10 μL) of a radiolabeled solution (³³P, about 30 μCi per plant) was put onto the punctured area.

3) The coleoptiles of the last two plants were punctured with a tip of a pair of tweezers and a droplet (10μL) of a non-acidic (pH of water, *i.e.* about 5.6) radiolabeled solution (³³P, about 30 μCi per plant) was put onto the punctured area.

For all three methods an activity of about 30 μCi per plant was used.

After trying these different methods of plant labeling, eventually labeling method 3) was chosen. This is because it gives more control on how much of the labeling solution is actually applied and because it is conducted much easier than 1); and it is because there was no advantage of 2) over 3) though both, 2) and 3) worked equally well.

2.5.1.2. Whole plant autoradiography

One day after labeling, the plants were harvested. The distribution of the radioactive phosphorus throughout the whole plants was checked using digital autoradiography: the plants were removed from their hydroponic vessels and put onto autoradiography plates that were covered with aluminum foil.

For this experiment phosphorimaging autoradiography was chosen as the method for imaging. Phosphorimaging is a form of solid-state liquid scintillation. Autoradiography plates used for this kind of autoradiography are coated with photostimulable crystals; when the

⁷ See appendix for list of nutrients added to the hydroponic solutions.

plate is exposed to a sample containing a radioisotope, the radiation emitted excites electrons in the crystal material. The electron is trapped within *e.g.* bromine vacancies in the crystal until exposed to visible light at a specific wavelength; this exposure releases the trapped electrons from the vacancies, allowing the excited crystals to return to their ground state, causing photons to be released at a different wavelength. This emitted light can be recorded by a digital scanner device. After the scanning of the autoradiography pictures, the plates can be erased by exposure to visible light (Johnston et al. 1990; Kanekal et al. 1995). Therefore, the plates are reusable.

2.5.1.3. Two-dimensional ³³P-sampling tests

Preliminary 2D efflux experiments with elaborated procedures as mentioned above with soil rhizotrons and one Gelrite rhizotron were conducted more to check the utility and the feasibility of the whole experiment than to take a closer look at some details or at the final set of data.

So a set of 12 rhizotrons with soil treatments as described in 2.1.1 and 2.4 (3 rhizotrons with +P Forchtenstein, 3 with –P Forchtenstein, 3 with +P Santomera, and 3 with –P Santomera) was prepared. Instead of the PTFE foil underneath the top Plexiglas plate, the open side of the rhizotrone was covered with a membrane (Whatman Nucleopore, 0.2 µm pore size). After six days of plant growth only 4 rhizotrons could be used for the DGT sampling (the others did not provide proper sampling sites around plant roots). These were R1, R2, R3, and R4. All of these were filled with Forchtenstein, only R4 was a phosphorus deficient repetition. So no Santomera repetition could be tested in the preliminary experiments.

Following two basic ideas concerning the experimental design, a sampling setup with rhizotrons containing sterile (or at least antiseptic) gel as a growth medium was required. The ideas were to show that 1) root phosphorus efflux is not an artifact caused by root injuries due to soil compaction and root damage during DGT application and rhizotron handling and 2) that effluxed phosphorus is not an artifact caused by the zero sink quality of a DGT gel matrix. It is arguable though not to regard 2) as an artifact *a priori* if one just thinks about the sink qualities of soils, *i.e.* sorption, and the phosphorus demands of microorganisms, *i.e.* absorption. A soft and almost watery growing medium such as Gelrite or agarose reduces the mechanical pressure on the roots, allows for opening a rhizotron without injuries to the roots, and possibly allows to rule out that phosphorus is withdrawn from roots by the DGT only or excessively, if it is possible to establish evidence that

phosphorus efflux is not only directed towards the DGT but also away from the DGT gel into the agarose gel matrix, which does not function as a zero sink.

For all Gelrite/agarose experiments broader rhizotrons were used. On the bottom side of the filled rhizotrons a nylon membrane was applied (0.45 μm pore size, manufactured by BioBond), onto which the DGT gel could be put.

For both, the soil and the Gelrite rhizotrons, DGT gels were applied on appropriate areas of the root system, *i.e.* where many root tips and sections of the root axes were located. Then the plants were labeled with ^{33}P : while a droplet of 2 μL containing about 6 μCi in total was put onto the coleoptile of the plant grown on Gelrite, droplets of 6 μL containing about 14.3 μCi each in total were applied onto the coleoptiles of the plants grown on soil (Fig. 9). Two days later the DGT

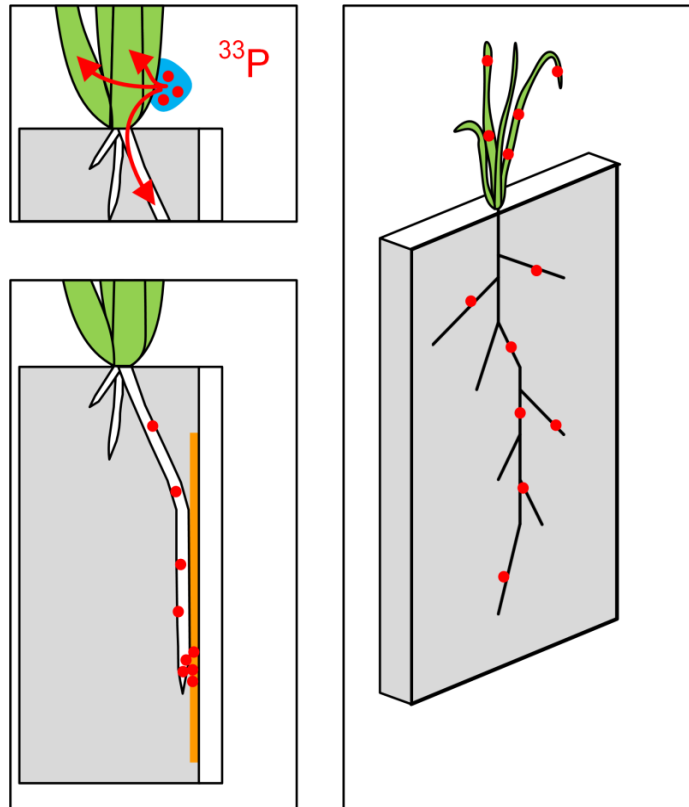


Figure 9 shows the basic scheme of the process of plant labeling with ^{33}P . Left top: a droplet of a certain amount and activity of the radiophosphorus is applied on a small lesion site on the coleoptiles. Left bottom: phosphorus and hence radiophosphorus is redistributed within the plant tissues; via phloem stream phosphorus reaches the root system. Right: after a certain period of time radiophosphorus can be detected everywhere within the plant. (Figure by courtesy of Jakob Santner)

gels were removed, the rhizotrons were wrapped in cling film and the whole root systems were exposed to the autoradiography screens. The DGTs were put onto aluminum foil,

bagged and then put into autoradiography cassettes. While the root system was left on the screens for two hours, the DGTs were left in the cassettes for 48 hours.

2.5.2. Main experiments

The main experiments were carried out in three series. The first series was done with Santomera soil, the second with Forchtenstein soil, and the third was done with agar nutrient gel as a growing medium. For the sampling procedure see 2.5.1.

2.5.2.1. Main experiments with soil rhizotrons

Main experiments with Santomera soil were conducted with rhizotrons named R7 – R12. Only R7 had to be removed because the seedling planted in it had died after the growing period of seven days. Then DGT gels were applied on appropriate positions of the root system on the membrane. After the application of the DGT gels the plants were radiolabeled by puncturing the coleoptile (Fig. 9) and applying a 3 μL droplet containing an activity of 19.2 μCi . 48 hours later, the gels were removed and each spread on a piece of aluminum foil (root exposed side facing up) and bagged in a plastic bag. The rhizotrons were wrapped in cling film and put onto autoradiography screens for exposure times of two hours. After the exposure the screens were scanned. The bagged DGT gels were also exposed to autoradiography screens. Afterwards the screens were scanned.

2.5.2.2. Main experiments with agarose rhizotrons

As almost all attempts to establish a procedure to fill rhizotrons with Gelrite and to grow maize plants in those rhizotrons (as described above) failed due to microbial colonization of the media, a standard procedure for the cultivation of plants under laboratory conditions was adapted and carried out in the laboratories of the research group of Professor Gerhard Adam at the Department of Applied Genetics and Cell Biology. According to this procedure the so-called “Very MS (Murashige and Skoog) Medium” (a modified Murashige and Skoog medium) was prepared for the main experiments with agarose rhizotrons. For each rhizotron 800 mL of Millipore water in Schott flasks was heated and stirred on heat plates and brought to the boil shortly, while to each solution 3.52 g of Murashige and Skoog salt mixture and 0.4 g MES were added. The pH was adjusted to 5.7 to 5.8 by addition of an appropriate amount of 1 mol L⁻¹ NaOH. Shortly before putting the flasks into the autoclave, 6.4 g agarose powder were added to each flask and mixed into the solution. The maize seeds were disinfected by washing in Millipore water containing 0.5 mL per liter of TWEEN 20 as a detergent to remove dust. Then the seeds were transferred to an autoclaved beaker. In the beaker the seeds were washed with 70% ethanol for five minutes by gently stirring. Then the ethanol was removed and a 3% hydrogen peroxide solution containing 0.5 mL per liter TWEEN 20 was added; the solution was stirred gently for another 15 minutes. After this time, the hydrogen peroxide was removed and the seeds were washed five times (in about 300 mL each) with sterile Millipore water for 5 minutes. All rhizotron parts were disinfected or sterilized as well as possible: the Plexiglas frame, the covering plates, and the clamps were

disinfected in a sodium hypochlorite solution ($\text{NaClO } 2.8 \text{ g L}^{-1}$) for about two hours. The Biobond and the Nucleopore membranes were immersed in a 70% ethanol solution for several hours. Sodium hypochlorite and ethanol were rinsed off properly with sterilized water. Blades and waterproof adhesive tapes were disinfected by exposition to ultraviolet radiation for about 15 minutes.

After assembling of the rhizotrons and autoclaving the agarose solutions for at least 40 minutes the gels were cast and allowed to cool. Then, five seedlings per rhizotron were planted into the gels with a sterilized pair of tweezers. After this the rhizotrons were sealed with parafilm and then transferred to a growth chamber. After three to five days of growth four of the five seedlings were removed. For the next two weeks the plants were allowed to grow at 20°C , 16 hours light per day, and 55% relative humidity. During the time of plant cultivation no indications of biological contamination were observed.

When the plants had reached the three leave stage, the coleoptiles of five plants were punctured and labeled with $19.176 \mu\text{Ci}$ in a $3 \mu\text{L}$ droplet (Rg) or with $14.985 \mu\text{Ci}$ in a $15 \mu\text{L}$ droplet (RA, RB, RC, and RD). Further sampling procedures were conducted as described in 2.5.1.

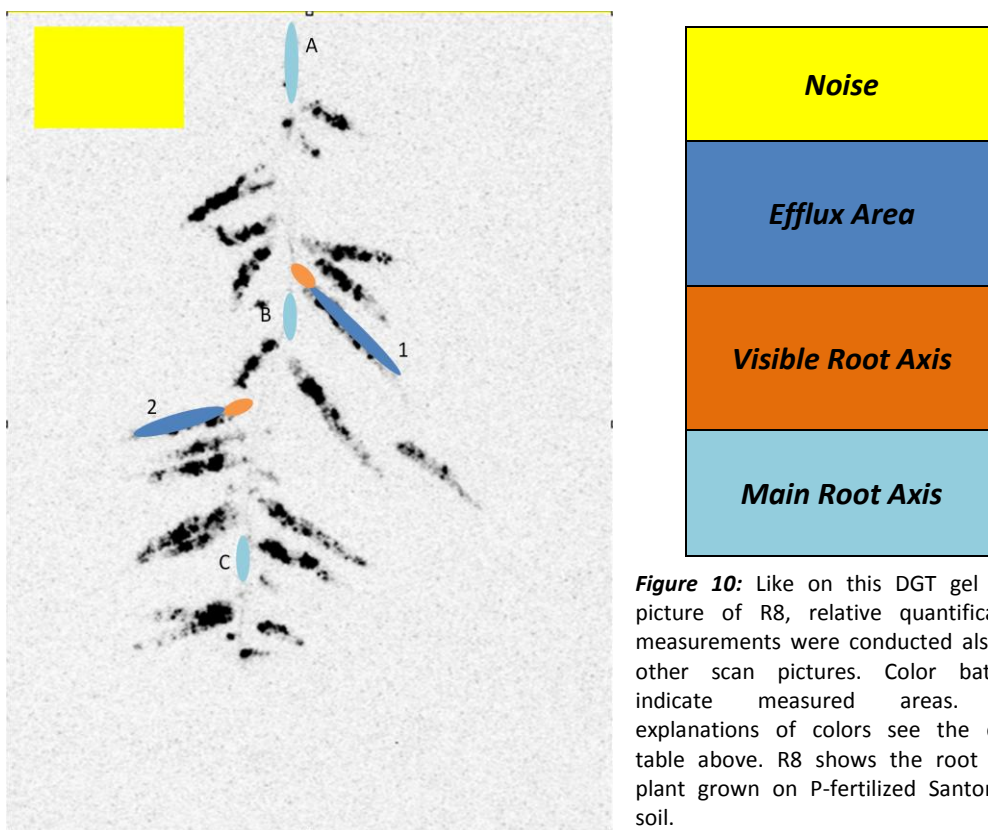
2.5.3. Relative root efflux analysis

2.5.3.1. Image calibration for relative efflux analysis

To be able to translate possible efflux grey value signals evident on DGT gel scans into values of radioactivity, a calibration function was determined. Therefore, ten standards were prepared by diluting the original spike with $1 \text{ mol L}^{-1} \text{ H}_2\text{PO}_4$ according to calculated dilution factors resulting in a maximum standard of about 4,000,000 and a minimum standard of about 20,000 CPM mL^{-1} . A droplet of $60 \mu\text{L}$ of each of these standards was pipetted on a $0.45 \mu\text{m}$ Whatman membrane disc resulting in ten discs soaked with different standard solutions. (The appropriate size of the droplet had been determined in preliminary experiments; the aim was to soak the entire disc but not to lose any solution by excess loading.) The remaining standard solutions were diluted and prepared for scintillation counting: $50 \mu\text{L}$ of the standards were mixed with $950 \mu\text{L}$ of water and $2,000 \mu\text{L}$ of scintillation liquid. The soaked discs were exposed to autoradiography screens for 48 hours and afterwards the screens were scanned.

2.5.3.2. Analysis of root axis/root tip ratio

For the analysis of the root axis to root tip ratio on the scan pictures of the DGT gels four different kinds of areas on the scan pictures were measured (see Fig. 10). The background noise was determined on completely unaffected areas. For the determination of the efflux areas clearly defined areas of P efflux were selected, ranging from efflux start to efflux end. For the measurement of the root axis efflux, visible and expected areas of root axis efflux, this is usually a thought line from the main root axis to the beginning of the efflux area at the root tip, were selected on the one hand; on the other hand, areas along the main root axis were selected.



The absolute CPM signals of the measured areas were divided by the number of pixels of the areas, resulting in average signals given as CPM per pixel. The values for the root axis and the root tip areas were noise corrected by subtracting the average CPM per pixel of the background noise area. For the calculation of the CPM per pixel values of the root tips, the noise corrected values were multiplied by the number of pixels covered by the area in

question and divided by an estimated area size of the root tip of 25 pixels. Then the signals per pixel of the root axis were divided by the signals per pixel of the root tip; for the percentage of the efflux of the root axis compared to the efflux of the root tip, the ratios were multiplied by 100. The way of calculation of the ratios can be formulated as follows:

$$(6) \quad ATR = \frac{\left(\frac{CPM}{p}\right)_{axis} - \left(\frac{CPM}{p}\right)_{noise}}{\left[\left(\frac{CPM}{p}\right)_{tip} - \left(\frac{CPM}{p}\right)_{noise}\right] \times p_{tip} \div 25}$$

where *ATR* means the root axis to root tip ratio, *CPM* means the absolute counts per minute values of the areas, and *p* means the number of pixels covered by the area.

3. Results and Discussion

3.1. ³¹P-efflux experiments

3.1.1. DGT standards for laser ablation ICP-MS

The prepared standards (as described in 2.4.2) were measured by colorimetric determination of phosphorus after elution and by LA-ICP-MS (results as mean ratios of ³¹P/¹³C). The blank-corrected P loading values, given as P $\mu\text{g cm}^{-2}$, were used for the calibration ratios between phosphorus loading on the one hand and LA ICP-MS data on the other hand. These ratios, *i.e.* calibrations between phosphorus loading of the standards and means of ³¹P/¹³C ratios were set up for each DGT separately. See appendix (6.2) for the individual calibrations.

Table 3 shows the P loading of the standard gel discs, given as values analyzed in the elution solution and as converted data for the whole discs. The weights of the halves were compared to the weights of the complete discs in order to calculate the phosphorus contents of the whole discs. Blank correction was carried out based on the P loading per cm^2 for the whole discs.

Calibration Standards - Data Table				
Standard #	Standard Name	Elution P $\mu\text{g L}^{-1}$	Absolute Disc P μg	Blank corr. P Loading $\mu\text{g cm}^{-2}$
1	1.1	64.1	0.076	0.013
	1.2	44.6	0.057	0.007
2	1.3	178	0.197	0.051
3	2.1	119	0.151	0.036
4	2.3	165	0.170	0.043
5	3.1	271	0.304	0.085
6	3.3	401	0.456	0.134
7	3.5	564	0.706	0.213

3.1.2. Calibrated and scaled DGT pictures

Figures shown below were calibrated according to the calculated calibration lines shown in the appendix (6.2), and the pictures were scaled according to the actual reading resolution, as pictures are delivered with square pixels, but actual reading points are rectangular ($x=132\mu\text{m}$, $y=350\mu\text{m}$). For all the following figures calibration bars are attached showing

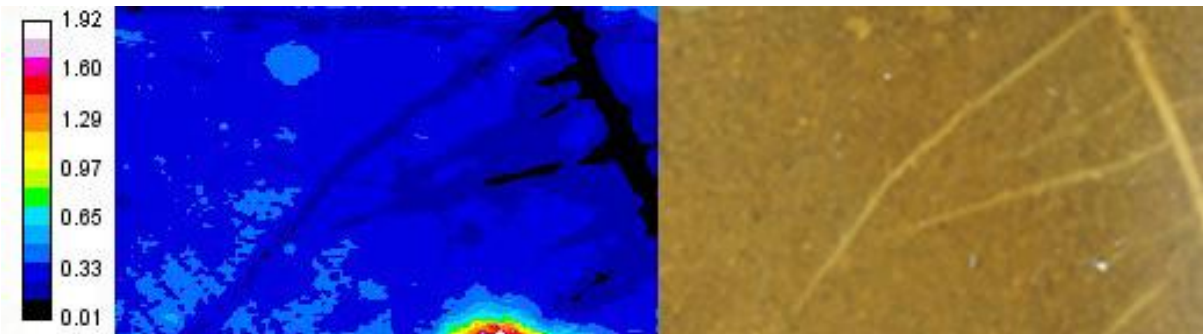


Figure 11: F1R2: Forchtenstein, P-fertilized. Dark areas at sites were root axes have to be expected (according to photo at the right side) indicate a clearly visible depletion zone. A red color batch at the bottom shows an artifact due to sampling difficulties. Values of the calibration bar are given as $\mu\text{g P cm}^{-2}$.

Figure 12: F2R1: Forchtenstein, P-unfertilized. Again the depletion zone is clearly visible. A red color batch in the lower area again shows an apparent artifact due to sampling difficulties, also gel cracks – appearing green to yellow – through this red area with the highest P values can be seen. The black areas show air bubbles between DGT gel and soil (see photo on – these bubbles can also be seen on the photograph. Values of the calibration bar are given as $\mu\text{g P cm}^{-2}$.

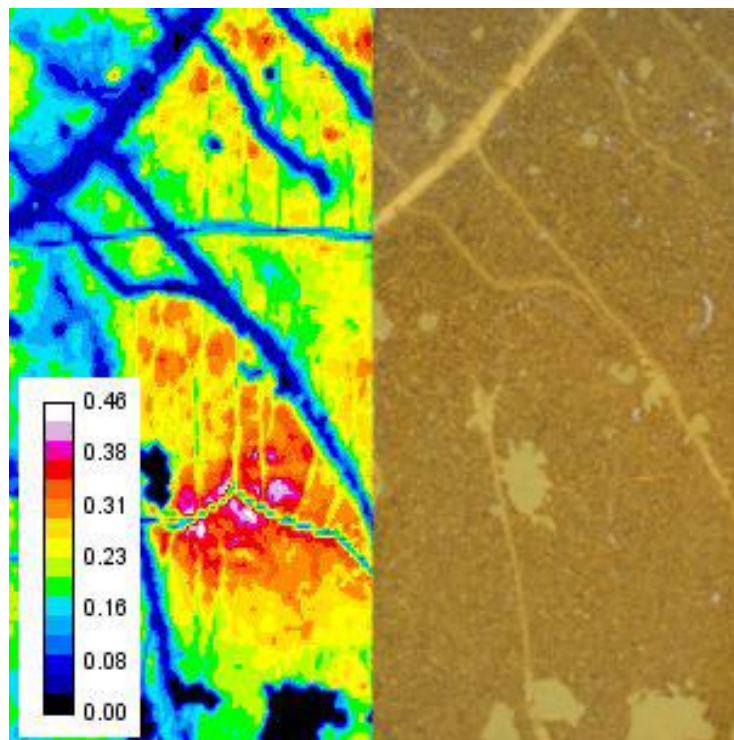


Figure 13: S1R2: Santomera, P-fertilized. In the upper middle white to red to green phosphorus hotspots are visible. Values of the calibration bar are given as $\mu\text{g P cm}^{-2}$. The black areas in the lower half appear to depict air bubbles during sampling procedure, *i.e.* areas where there was no contact between soil and DGT gel.

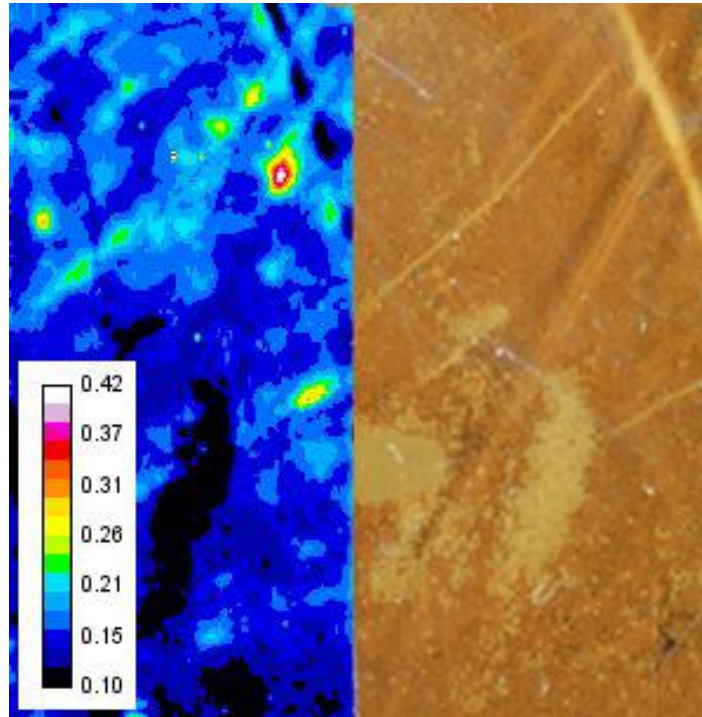
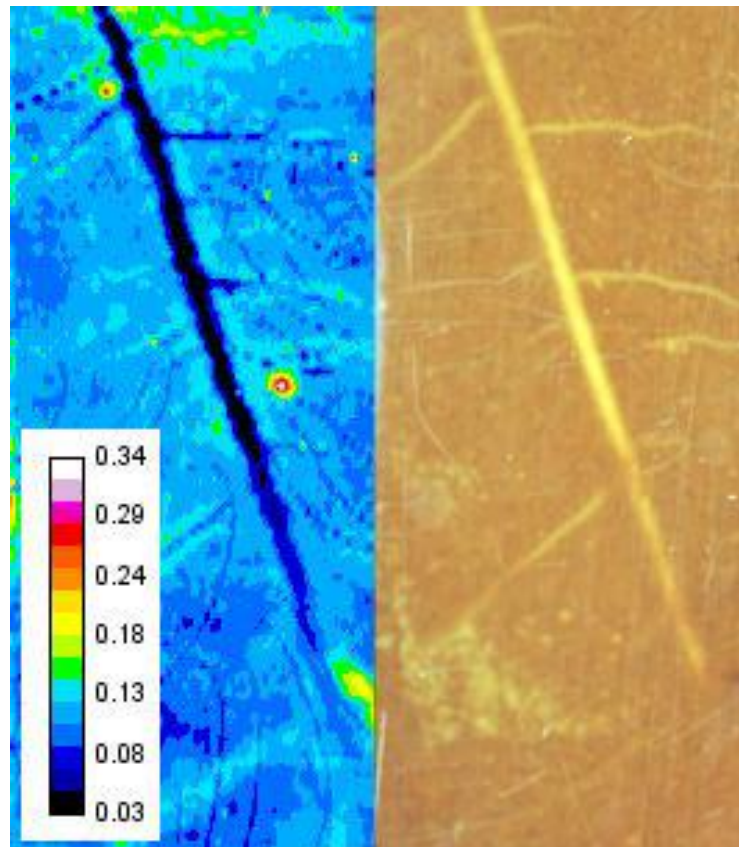


Figure 14: S2R1: Santomera, P-unfertilized. At the upper left and in the middle on the right of the depletion zone phosphorus hotspots are visible. Values of the calibration bar are given as $\mu\text{g P cm}^{-2}$.



3.2. ³³P-efflux experiments

The following pictures show from left to right: photo taken before sampling, DGT scan picture after 48h, root scan picture at the end of sampling period, and photo taken at the end of sampling period – this order is the same for all following picture alignments of this sort.

3.2.1. Preliminary experiments

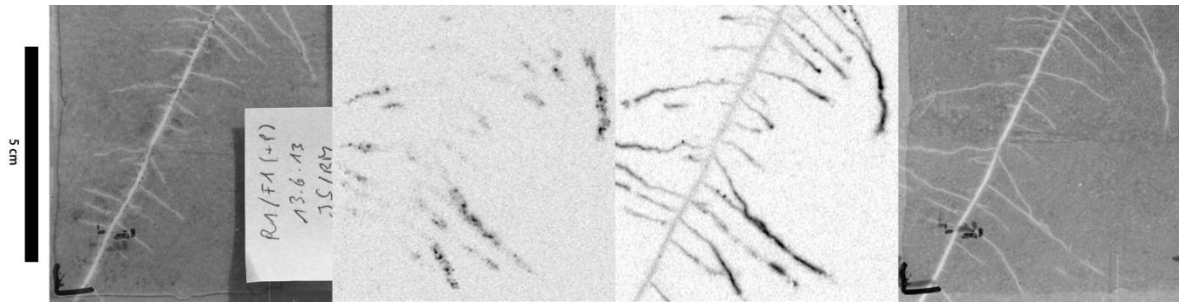


Figure 15: R1F1

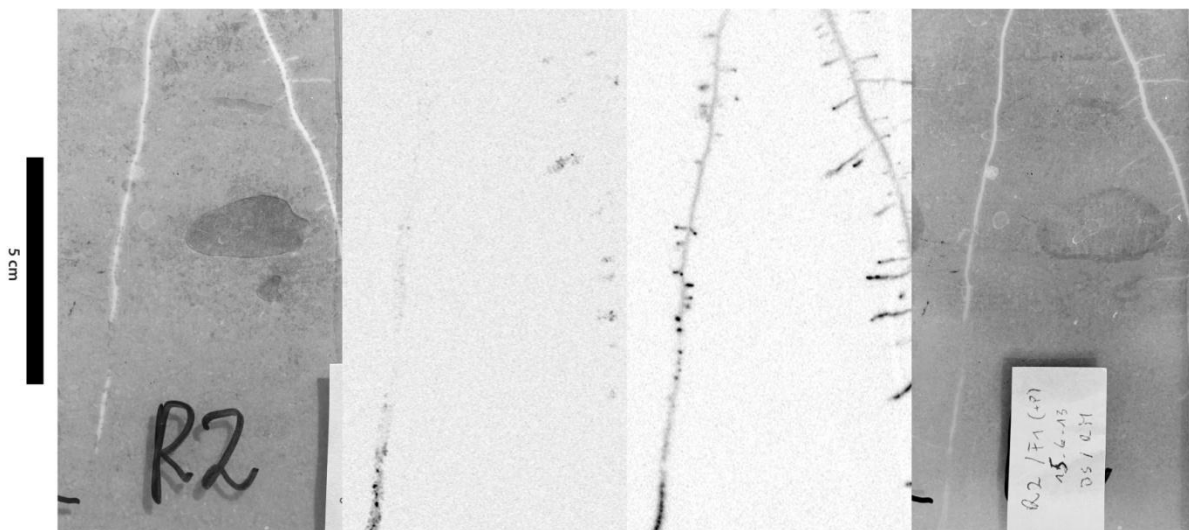


Figure 16: R2F1

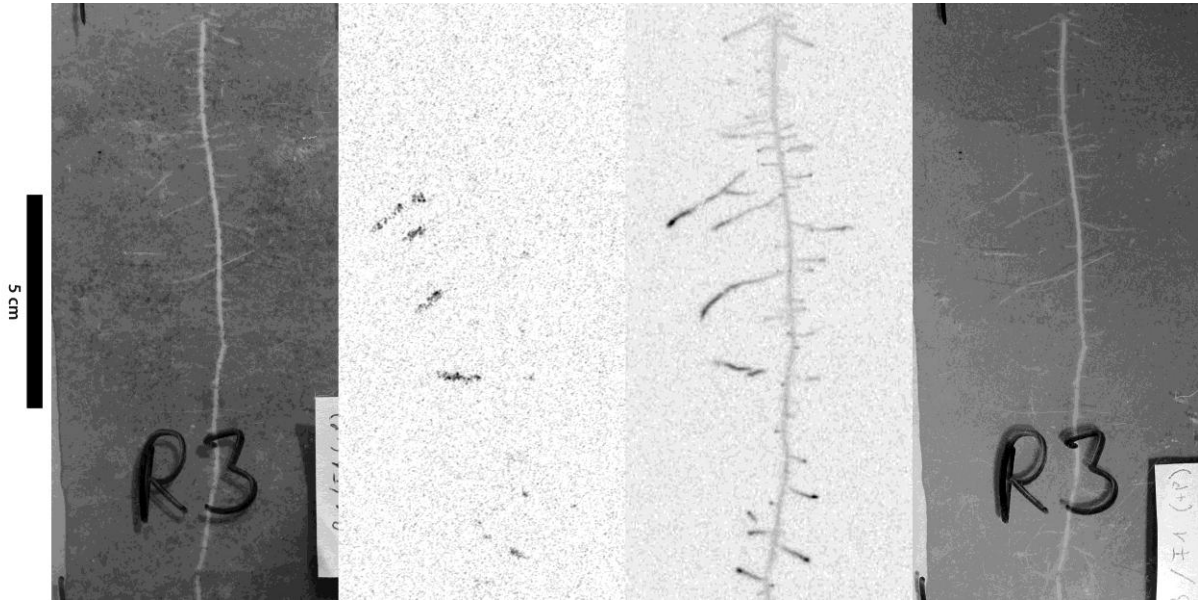


Figure 17: R3F1

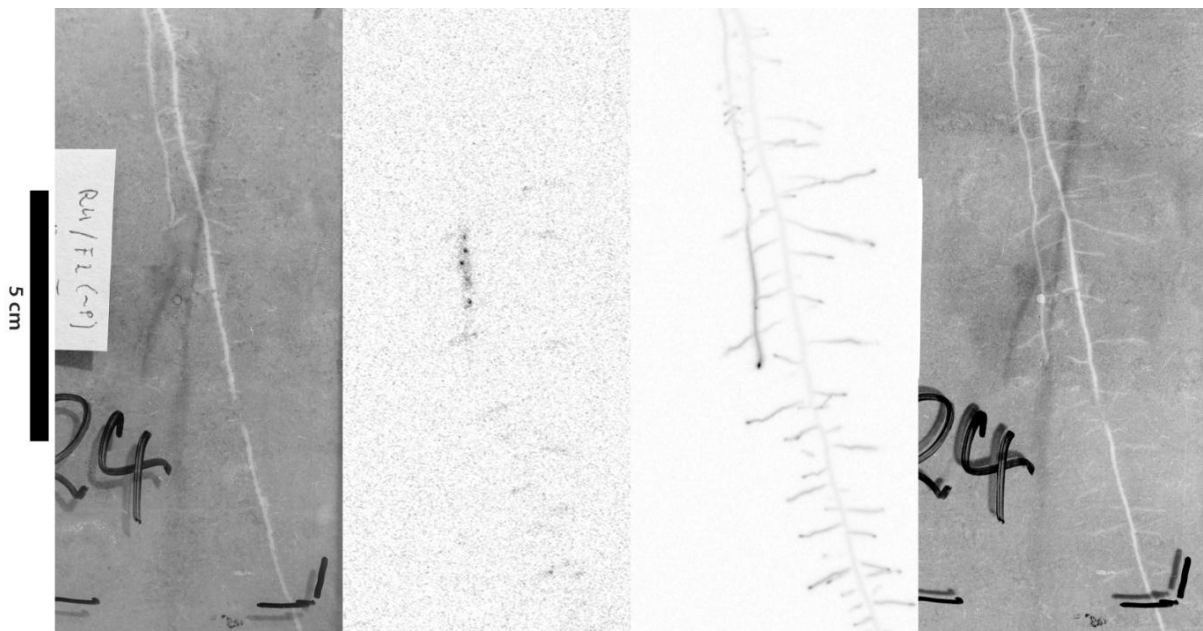


Figure 18: R4F2

On all above depicted DGT gel scan pictures (Fig. 15 – 18) efflux sites at root growing sites and root tips are clearly visible. When looking at the left side of the DGT scan in Fig. 16, strong efflux activities can be seen along the root prolongation zone on a distance of about 2 cm. The same becomes visible when looking at the DGT scan of Fig. 18, where a trace of efflux is also spread on the distance of about 2 cm.

3.2.2. Soil Forchtenstein

3.2.2.1. With phosphorus fertilization

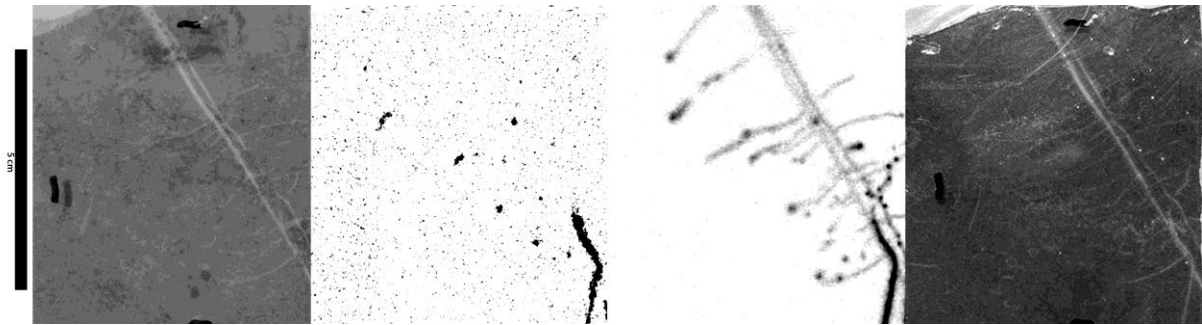


Figure 19: R2

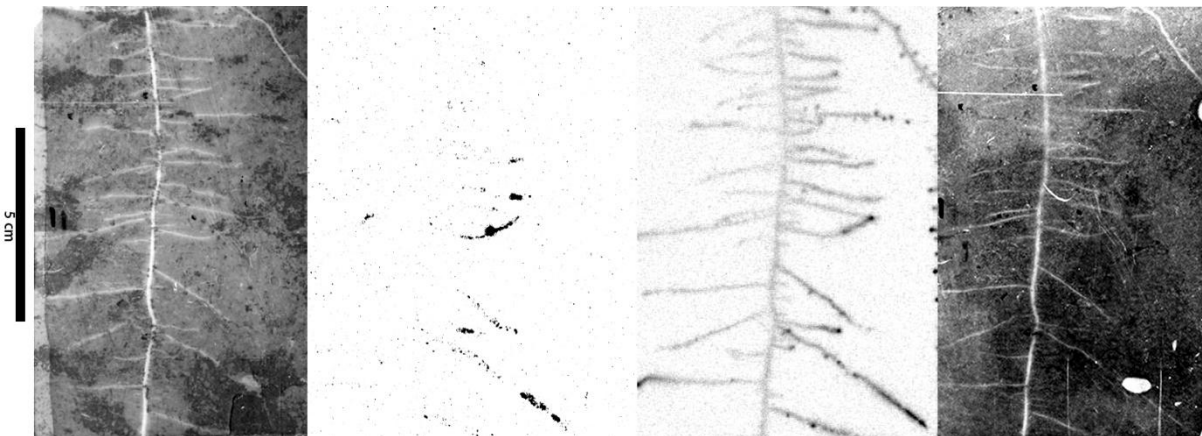


Figure 20: R3

3.2.2.2. Without phosphorus fertilization

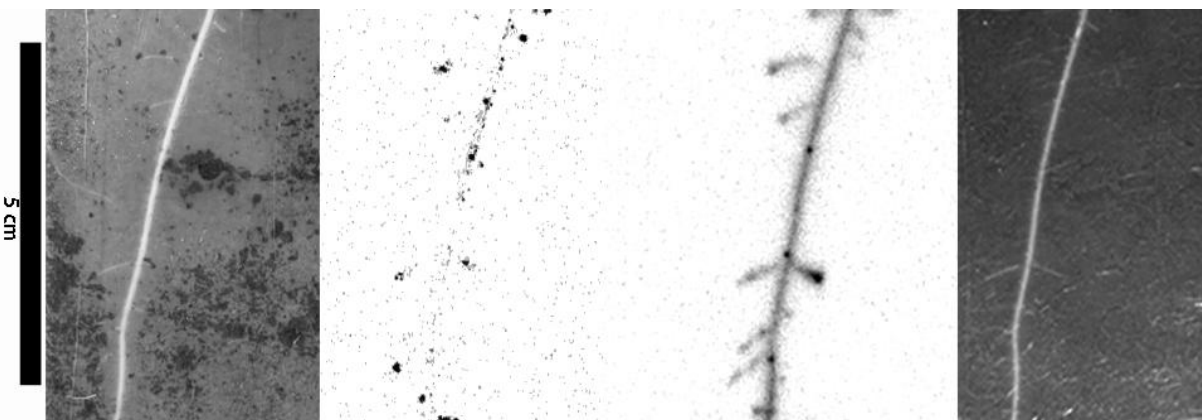


Figure 21: R5

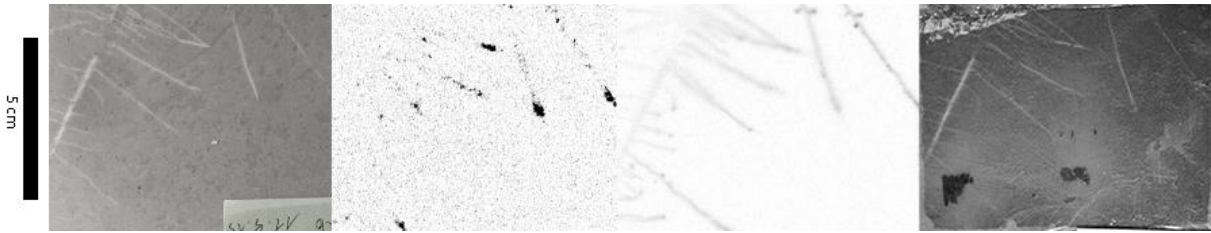


Figure 22: R6

Also on the pictures of Fig. 19 - 22 efflux sites with a clear emphasis on the root tips are visible.

3.2.3. Soil Santomera

3.2.3.1. With phosphorus fertilization

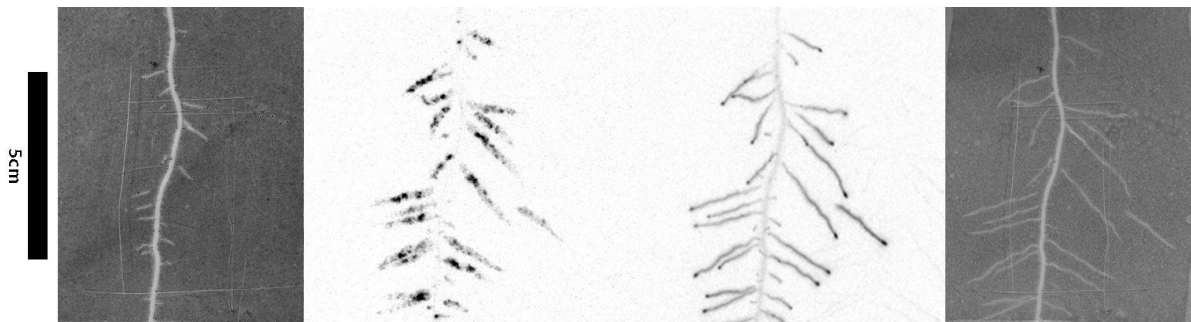


Figure 23: R8

That root efflux apparently comes along with root growth can be interpreted when looking at the “detached” root on the right side in the middle of the DGT scan picture of Fig. 23: while not visible on the first photo, the root grows “into the picture” and thereby leaves a trace of radiophosphorus along its growth on the DGT device. Besides that, Fig. 23 - 27 are very similar to the pictures in the sections above (3.2.1, 3.2.2).

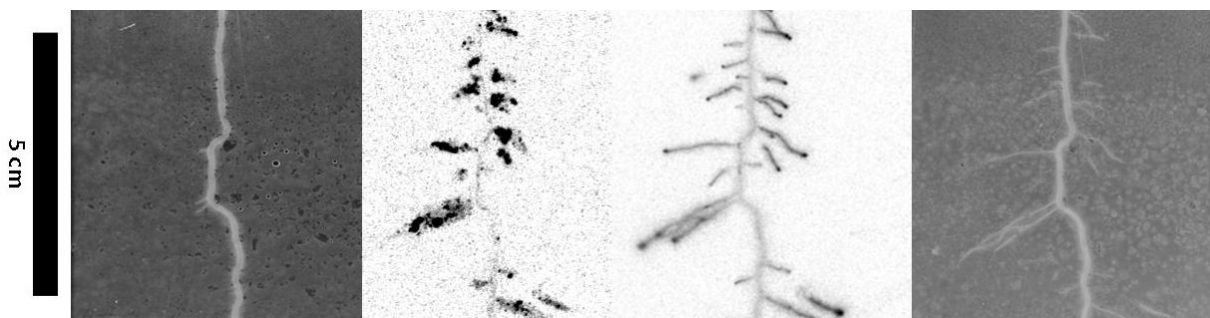


Figure 24: R9

3.2.3.2. Without phosphorus fertilization

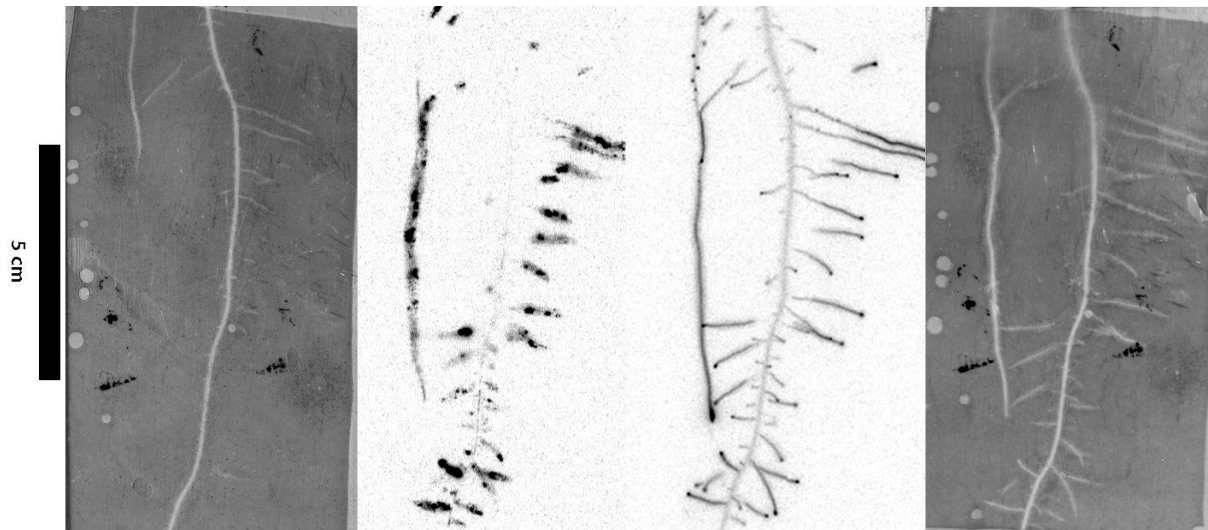


Figure 25: R10

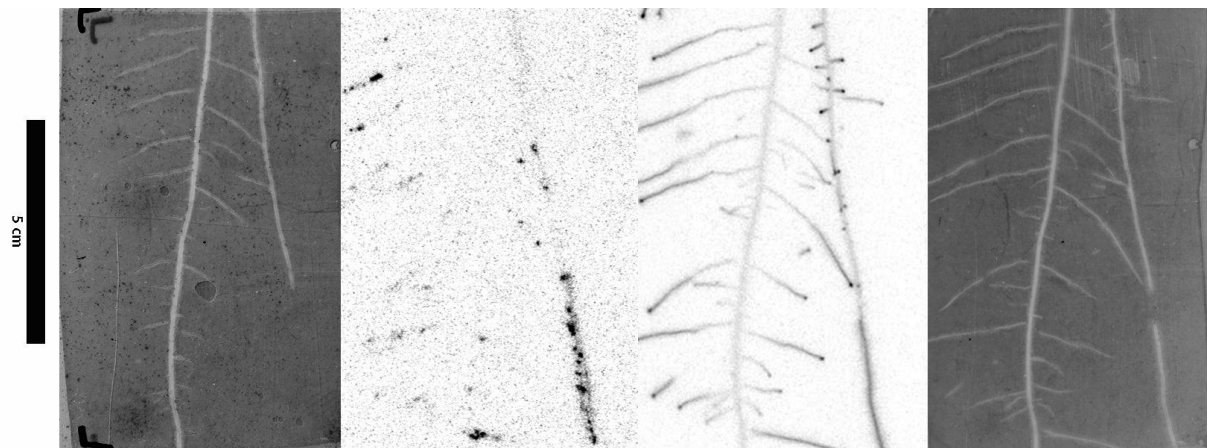


Figure 26: R11

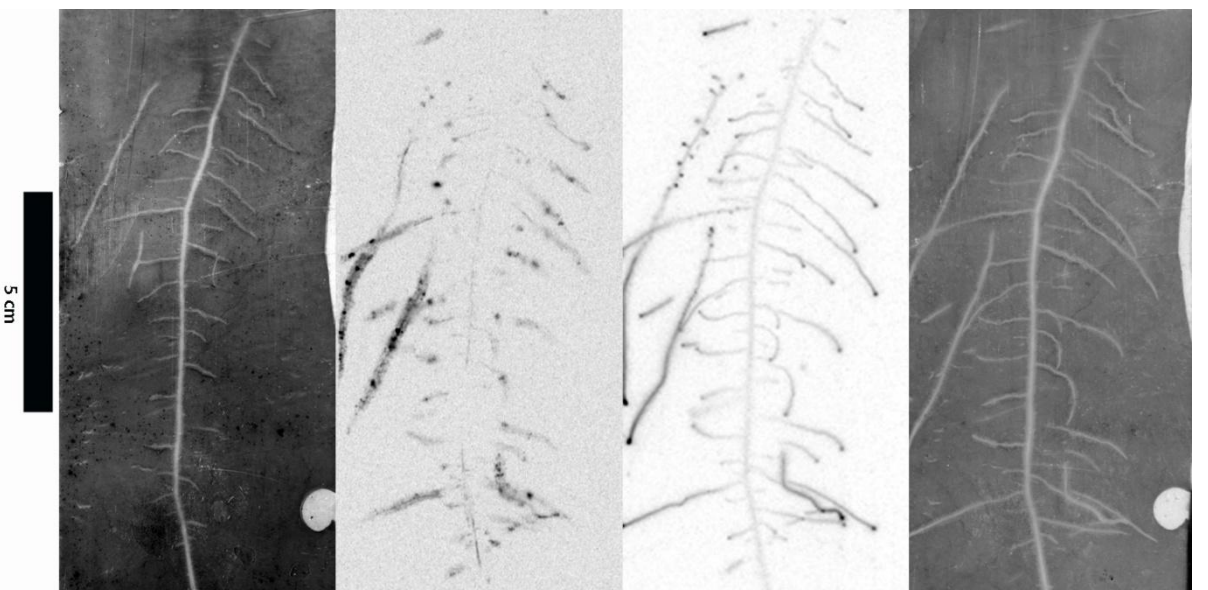


Figure 27: R12

3.2.4. Gelrite/agarose gel

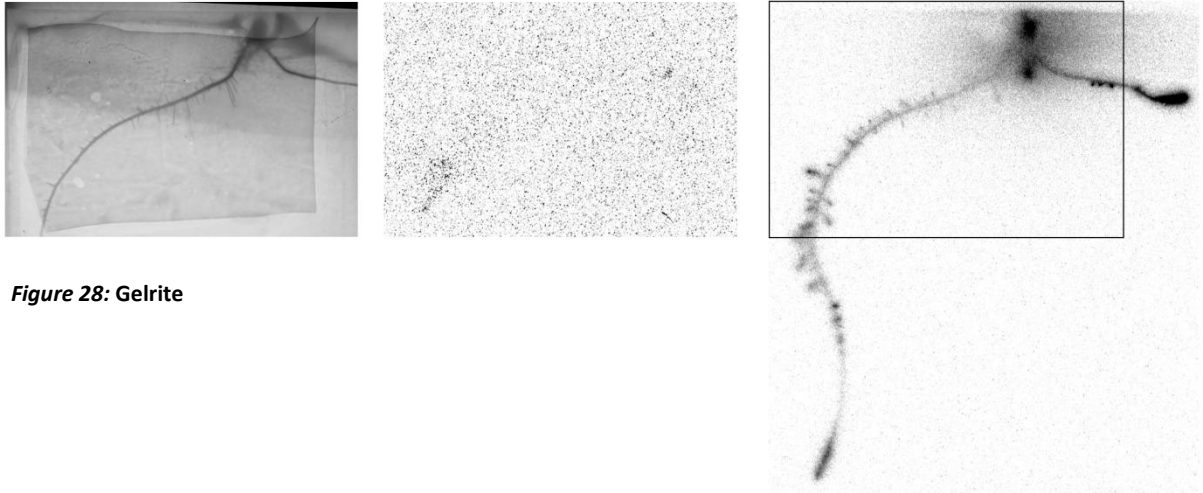


Figure 28: Gelrite

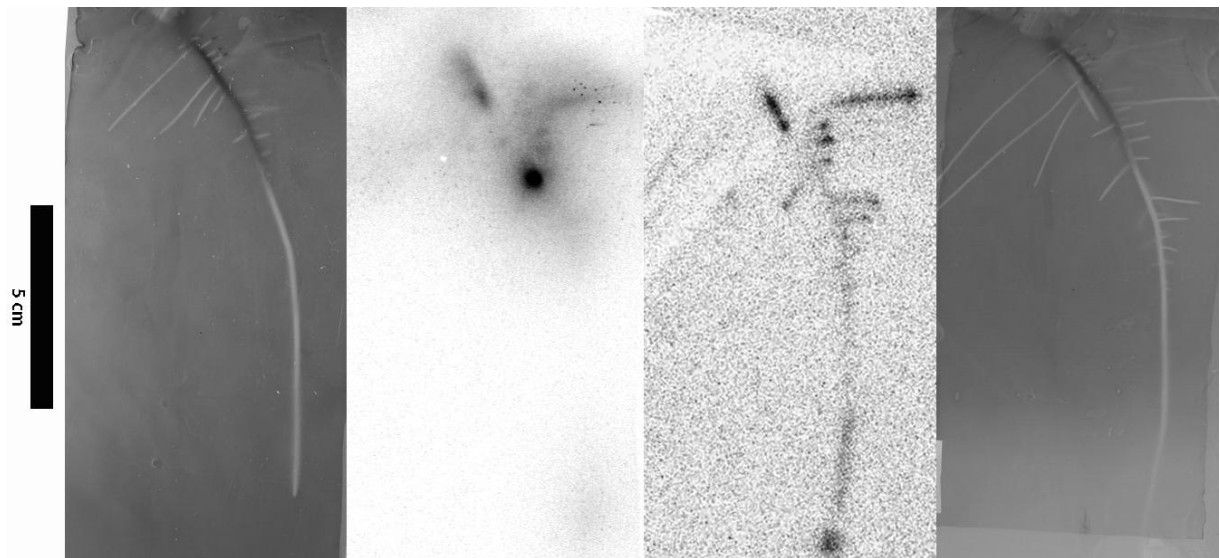


Figure 29: Rg

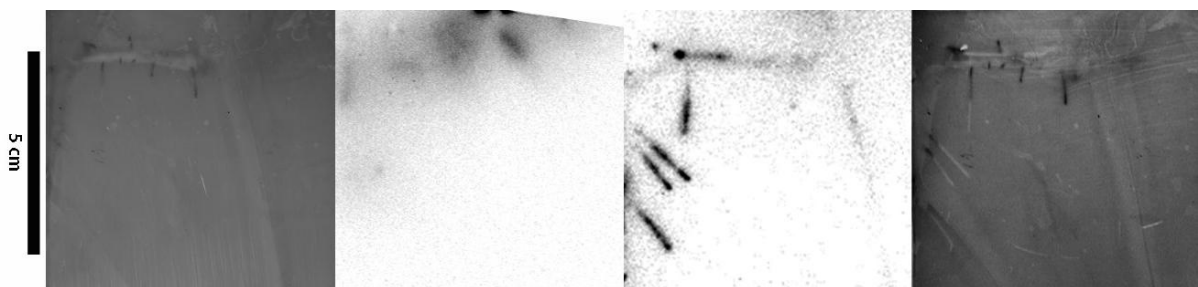


Figure 30: RA

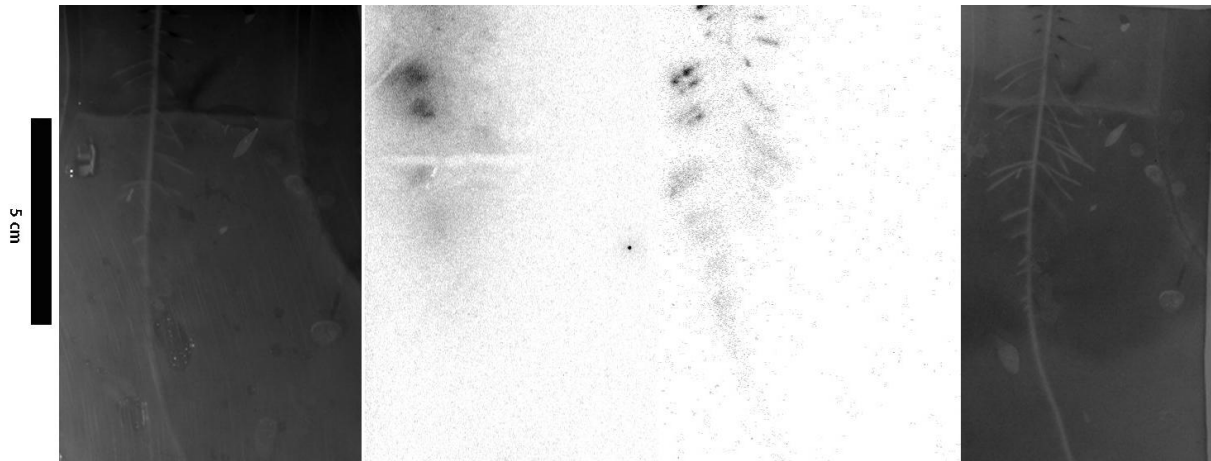


Figure 31: RB

The first successful experiment on a non-soil-medium and one of the first successful radiophosphorus efflux experiments of this kind at all was carried out with a Gelrite rhizotron treatment. One can see (although hardly) efflux spots on the DGT gel scan picture of the Gelrite treatment (Fig.28). A photo after the sampling period is missing.

The DGT gel scan picture of Rg (Fig. 29) was the first picture with the “³³P-cloud” becoming clearly visible around the efflux areas. This diffusion cloud is also clearly visible on the scan picture of Fig. 31; it also shows fluent shades of grey values within the cloud that correlate to the differently active areas depicted in the whole root scan picture.

3.3. Root axis to root tip efflux ratios

3.3.1. Image calibration: grey values vs. ^{33}P -activity

Table 4 shows the scintillation counting results of the standard series put up for the calibration of the root and the DGT gel scans after sampling. Membrane discs were soaked with different dilutions of radiophosphorus solutions. These solutions were analyzed by scintillation counting and related to disc area.

Standards Scintillation Counting Results			
Standard #	blank corrected CPM	CPM mL ⁻¹	CPM cm ⁻²
I	37500	5000000	61100
II	30000	4000000	48800
III	26800	3570000	43600
IV	23300	3100000	37900
V	18400	2460000	30000
VI	13200	1760000	21600
VII	8840	1180000	14400
VIII	4520	602000	7360
IX	2900	116000	1420
X	1170	23400	286

Table 5 shows the grey value measurements of the standard series put up for the calibration of the root and the DGT gel scans after sampling. Membrane discs were soaked with different dilutions of radiophosphorus solutions. These solutions were analyzed by scintillation counting and related to disc area.

Standards Grey Value Measurement Results					
Standard #	blank corrected mean grey intensities	standard deviation (% on the right)		Min.	Max.
I	9900	189	1.8	9100	11000
II	9010	227	2.4	7970	10200
III	8710	215	2.3	8070	9980
IV	7750	225	2.7	7470	8880
V	6650	164	2.3	6430	7540
VI	5900	162	2.6	5480	7400
VII	4490	154	3.1	4030	5450
VIII	2880	128	3.9	2690	3780
IX	1260	113	6.7	1250	2160
X	388	115	13.9	400	1310

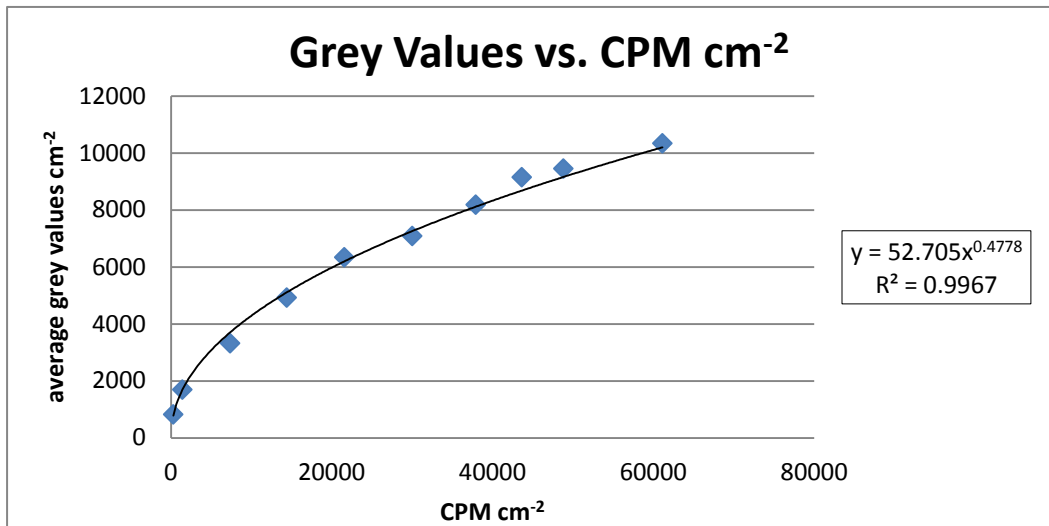


Figure 32: Grey values and CPM cm⁻² do not correlate in a linear way.

Thus grey values of the measured samples using digital autoradiography correlate to surface area-based CPM values according to the following non-linear equation obtained from the plot in Fig. 32:

$$y = 52.705 * x^{0.4778} \rightarrow x = \sqrt[0.4778]{\frac{y}{52.705}}$$

Therefore grey values in the pictures obtained by scanning the autoradiography screens were converted accordingly. As the resolution of the autoradiography scans is 200µm squared (200µmx200µm = 40000µm² = 0.0004 cm² equals one pixel), the calibrated grey values delivering CPM per cm² have to be divided by 2500 in order to obtain CPM per pixel.

3.3.2. Analysis of root axis/root tip efflux ratio

Table 6 shows the overall mean root axis to root tip efflux ratio obtained from the tables shown above.

Rhizotron #	axis/tip ratio	mean axis/tip ratio	axis/tip %
R3	0.014	0.0118	1.18
	0.0096		
R6	0.00332	0.00386	0.386
	0.0044		
R8	0.001	0.00068	0.068
	0.00036		
R9	0.005	0.008	0.8
	0.011		
R10	0.00296	0.0018	0.18
	0.00063		
R11	0.00796	0.00796	0.796
R12	0.00294	0.00232	0.232
	0.00170		
Overall mean axis/tip ratio	0.003		0.3

Table 7 shows the mean root axis to root tip efflux ratios for each treatment (*i.e.* soil X fertilization).

	mean axis/tip percentage %	standard deviation %
F -P	0.39	0.08
F +P	1.18	0.31
S -P	0.32	0.28
S +P	0.43	0.47

3.4. Discussion

3.4.1. ³¹P-efflux experiments

When looking at the four pictures (Fig. 11 – 14) obtained by the application of DGT gels onto the root-soil-interfaces of rhizotrons and the following LA-ICP-MS procedure, clearly on every picture depletion zones along the root axes can be seen. Those depletion zones appear as dark to black zones congruent with the root axis areas on the photos next to the LA-ICP-MS pictures. The LA-ICP-MS pictures of Fig. 11 and Fig. 12 show artifacts, apparently the sampling procedure did not work properly, no expected results can be shown by these pictures. Obviously on the pictures of Fig. 13 and Fig. 14 not only the depletion zones are depicted clearly, but also several phosphorus hotspots, *i.e.* spots of elevated phosphorus concentrations (about 0.2 to 0.4 $\mu\text{g cm}^{-2}$ P) can be identified. As it is known from literature (*e.g.* Emmert 1959; Elliott et al. 1984; Cogliatti et al. 1990) phosphorus efflux occurs, but direct two dimensional observations of possible phosphorus efflux hotspots were first reported by Santner et al. (2012). However, according to the latter reference both, the soil and the plant could be the source of the elevated P concentrations within the depletion zones. One possibility is that root exudates like citrate or mucilage-derived surfactants or the high release of H^+ enhance the solubilisation of phosphorus adsorbed to soil particles or precipitated phosphorus. Another possibility for the increased P concentrations is sloughed-off root cap cells that function as mechanical protection of the root as it elongates through the soil. After the death of these cells and their lysis P could be released into the soil solution. A third potential explanation for the P hotspots is direct efflux of phosphorus from the root into the rhizosphere.

As a consequence of these results and the fairly strong indications in the literature that efflux might be the reason combined with the importance of the efflux of phosphorus in the process of P uptake and nutrition as shown by kinetic uptake models, P efflux experiments with radioactive ³³P using the DGT method were designed and conducted.

3.4.2. ³³P-efflux experiments

3.4.2.1. Experiments with soil

According to the expectations well-founded by literature, the autoradiography exposures of the whole root systems done shortly after the removal of the DGT gels show the distribution of the radioactive phosphorus throughout the entire root system. Increased concentrations of radiophosphorus appear at the root tips and relatively equal concentrations across the

rest of the roots. This evidently establishes proof for the fundamental benefit of the chosen labeling method. Obviously the redistribution of phosphorus from aerial parts of the plant such as the coleoptile into the roots via phloem does not only work very efficiently but also fast. Unfortunately it cannot be said how the distribution looked like at the beginning of the sampling period and how it developed over this time. The accumulation of radiophosphorus in the root tips apparently goes along with an increased turnover of physiologically relevant phosphorus compounds in these tissues. The root tips are the sites of root growth and root elongation; while to the back side of the root apical meristem the actual root elongation occurs by producing cells for the bulk root body, to the front side the so called calyptra is formed. The calyptra is the root cap, which is made up of short lived cells that massively exude pectin (mucigel). The calyptra serves therefore as a mechanical protection of the easily vulnerable root meristem and enables the root to easily penetrate the soil. Major genetic and physiological processes in these areas are: *transcription* comprising the initiation of transcription (mainly based on mRNA synthesis), the mRNA elongation (dependent on GMP and GTP) and transcription termination (GTP-intensive processing of mRNA); *translation* comprising initiation of translation (building of initiator-tRNA) and decomposition of mRNA, phase of elongation (GTP/ATP-intensive, aminoacyl-tRNA and tRNA-involving processes) and phase of termination (GTP-intensive); other protein and cell building processes are *e.g.* the *modification* and the *folding* of proteins, the control of cell cycles, the distribution of proteins within the cell, etc. which are all highly dependent on energy obtained from ATP (Bresinsky et al. 2008). As one can see easily, the more active a cell is, the higher the phosphorus turnover becomes. This strongly increased cell activity is certainly the reason for the (compared to the other parts) accumulation of radiophosphorus in the root tips.

Also according to root efflux experiment literature, the pictures obtained by autoradiography exposure of the DGT gels that were applied onto the root-soil interfaces clearly show that phosphorus was effluxed from the roots. But even though the efflux evidence might have been expected from what had been reported by others, nevertheless the direct proof and the clear two-dimensional evidence of it are new. Apparently for the first time, in combination with the photographs taken at the beginning and at the end of the sampling period, it can be said that the efflux of phosphorus mainly occurs at the growing areas of the roots, *i.e.* at the root tips, as on the DGT gel scans growth traces can be clearly

localized. These growth traces are traces of phosphorus efflux that are captured on the DGT gels.

As already incorporated P is released into the rhizosphere via the root tips of maize, questions concerning the P use and acquisition efficiency do arise. It seems reasonable to assume that this efflux leads to a decrease of acquired and hence usable P supplies for the plant, even though a big part of the once released P is probably re-acquired by the root hair zone that develops next in the area of previous P efflux in the rhizosphere. Released P cannot be used by the plant for other purposes as long as it is outside of the plant and a decreased efflux of P means a higher P acquisition efficiency. Thus, plants with releasing less P might be in the ascendancy over plants with worse P use and acquisition efficiency. This could be a point worth a consideration in future plant-soil science and plant breeding.

Another point worth a consideration for future research is certainly the ecological role of P efflux. As temporarily increased P concentrations in certain sections of the rhizosphere do occur, microbial growth might be enhanced and it is imaginable that certain forms of rhizosphere symbiosis are triggered by plant P efflux. Contrary to reasonable assumptions of P use and acquisition efficiency as discussed in the previous paragraph, plants with increased P efflux might thereby even gain advantages over plants with reduced P efflux due to ecological deficiencies. Either way, the question of the role of P efflux and its possible benefits for the plant are certainly important topics for future research.

3.4.2.2. Experiments with agarose media

The DGT gels applied onto the roots grown in Gelrite or agarose gel also show clear efflux. However, the obtained pictures differ from those obtained when grown in soil. The major difference is that instead of clearly identifiable root tips or defined areas of root growth a cloud of efflux around the roots becomes visible. This is because in the agarose medium phosphate can easily diffuse into the matrix of the medium without being adsorbed to solid surfaces or being incorporated by any microorganism as the plants were sown under sterile conditions and grown under antiseptic conditions (as there are endophytes within the seeds that cannot be removed without causing harm to the plant embryo and that might start to grow as seeds start to germinate). Diffusion in the agarose medium is only limited by the diffusivity of phosphate in the gel, which is only slightly smaller than in water due to increased tortuosity. Therefore, not only phosphorus from close vicinity to the applied DGT diffused into the DGT but also from areas somewhat more deep and back in the agarose

matrix. As a result of this, the mentioned efflux clouds can be seen on the scans of the DGT gels applied on roots grown in this medium.

In conclusion, the effluxed phosphorus is not withdrawn from the root excessively, neither by the growing medium nor by the sampling DGT gel. The reason for this is simple: first, as there are no soil particles and there is no zero sink in the agarose gel, withdrawing of phosphorus from the root appears unlikely; second, as obvious radiophosphorus clouds appear on the DGT scan pictures, evidently the radiophosphorus first diffused into the medium (seemingly in all directions) and only later into the DGT strip; therefore, phosphorus efflux does not only occur due to withdrawing effects of the DGT gel. The possibility that the phosphorus appearing on the DGT strip is leaked into the medium due to mechanical root injuries caused by the movement of the root during the penetration of the growing medium can also be neglected as Gelrite and agarose hardly provide any mechanical resistance. Microorganisms as the reason for phosphorus efflux can also be ruled out, because the Gelrite/agarose media were sterilized.

3.4.3. Root axis to root tip efflux ratios

Direct localization of efflux sites in the root system allows the calculation of ratios of efflux between morphologically and physiologically different sites of a root system. We show that large differences exist between the efflux of main root axes and root tips. The average axis/tip percentage of all rhizotron treatments is 0.30% which means that only 0.30% of the radiophosphorus effluxed at the root tips is effluxed along the root axis. Between the four treatments efflux ratios seem to differ between Forchtenstein without phosphorus fertilization with a ratio of 0.39% (standard deviation: 0.08%) and the ones with phosphorus with a ratio of 1.18% (standard deviation: 0.31%); however, ratios appear not to differ between the Santomera treatments: Santomera without phosphorus 0.32% (standard deviation: 0.28%), Santomera with phosphorus 0.43% (standard deviation: 0.47%).

4. Conclusion

Looking back at the objectives set in the beginning, the following (indicated by paragraphs below numbers) can be said step by step; we wanted

1. to investigate the source of possible P hotspots at the root tips that were observed in Santner et al. (2012) using DGT-LA-ICP-MS chemical imaging. Potential sources are P solubilization from the soil as well as P efflux from plant roots;
 - As the radiophosphorus was applied at the coleoptile, an aerial part of the plant, and as it showed up on the DGT gel scans, it can most clearly be said that the plant tissues are the source of the effluxed phosphorus.
2. to make sure that the possibly observed phosphorus efflux does not occur due to root injuries;
 - As the DGT scan pictures of the roots grown in the Gelrite/agarose media show non-defined, diffuse efflux areas (“efflux clouds”), phosphorus appears to have effluxed into the media first and then to have diffused into the DGT strip. This rules out that the phosphorus is withdrawn from the root only or excessively by the DGT gel.
 - As roots can penetrate the Gelrite/agarose media smoothly and almost without any mechanical resistance, root injuries are very improbable and hence the possibility of the phosphorus being effluxed due to injuries is very improbable either.
3. the relative quantification of root phosphorus efflux at different root segments along the root axis using autoradiography.
 - Phosphorus efflux from maize roots is highly localized – this appears to be a main finding of this thesis.
 - Relative quantification of effluxed phosphorus can be conducted. The total mean root axis to root tip percentage of phosphorus efflux is 0.3%. However, reliable statistical data on this matter has not been established in this thesis.

Generally it can be concluded that P efflux does occur in maize roots and that this efflux is highly localized and almost totally restricted to the root tips; a relative quantification of the root axis/root tip ratio is possible by means of autoradiography.

5. References

- BARBER, S. A.** 1995: *Soil Nutrient Bioavailability: A Mechanistic Approach*. 2. Aufl. New York: John Wiley and Sons.
- BLUME, H.-P.; BRÜMMER, G.; HORN, R.; KANDELER, E.; KÖGEL-KNABNER, I.; KRETZSCHMER, R.** 2010: *Scheffer/Schachtschabel. Lehrbuch der Bodenkunde*. 16. Aufl. Heidelberg: Spektrum Akademischer Verlag.
- BRESINSKY, A.; KÖRNER, C.; KADEREIT, J.; NEUHAUS, G.; SONNEWALD, U.** 2008: *Strasburger. Lehrbuch der Botanik*. 36. Aufl. Heidelberg: Spektrum Akademischer Verlag.
- CLAASSEN, N.; BARBER, S. A.** 1974: 'A Method for Characterizing the Relation between Nutrient Concentration and Flux into Roots of Intact Plants'; In: *Plant Physiology*, Vol. 54, p. 564–568.
- COGLIATTI, G. H.; SANTA MARÍA, G. E.** 1990: 'Influx and Efflux in Roots of Wheat Plants in Non-Growth-Limiting Concentrations of Phosphorus'; In: *Journal of Experimental Botany* (41), p. 601–607.
- DAVISON, W.; ZHANG, H.** 1994: 'In site speciation measurement of trace components in natural waters using thin film gels'; In: *Nature* (367), p. 546–548.
- ECKERT, R.; RANDALL, D.; BURGGREN, W.; FRENCH, K.** 2002: *Tierphysiologie*. 4. Aufl. Stuttgart: Georg Thieme Verlag.
- ELLIOTT, G. C.; LYNCH, J.; LÄUCHLI, A.** 1984: 'Influx and Efflux of P in Roots of Intact Maize Plants. Double-Labeling with ^{32}P and ^{33}P '; In: *Plant Physiology* (74), p. 336–341.
- EMMERT, F. H.** 1959: 'Loss of Phosphorus-32 by Plant Roots after Foliar Application'; In: *Plant Physiology*, Vol. Volume 34 (07), p. 449–454.
- EPSTEIN, E.** 1953: 'Mechanism of ion absorption by roots.'; In: *Nature* (171), S. 83–84.
- EPSTEIN, E.; HAGEN, C. E.** 1952: 'A kinetic study of the absorption of alkali cations by barley roots.'; In: *Plant Physiology* (27), p. 457–474.
- HINSINGER, P.** 2001: 'Bioavailability of soil organic P in the rhizosphere as affected by root-induced chemical changes: a review'; In: *Plant and Soil* (237), p. 173–195.
- JOHNSTON, R.; PICKETT, S.; BARKER, D.** 1990: 'Autoradiography using storage-phosphor technology'; In: *Electrophoresis* (11), p. 355–360.
- KANEKAL, S.; SAHAI, A.; JONES, R.; BROWN, D.** 1995: 'Storage-phosphor Autoradiography: A Rapid and Highly Sensitive Method for Spatial Imaging and Quantitation of Radioisotopes'; In: *Journal of Pharmacological and Toxicological Methods* (33), p. 171–178.
- KREUZEDER, A.** 2011: *Modelling Phosphorus Flows in Soils*. Master Thesis: Karl Franzens Universität, Graz. Institute for Chemistry, Institute for Systems Science, Innovation & Sustainability Research.
- MARSCHNER, H.; MARSCHNER, P.** 2012: *Marschner's mineral nutrition of higher plants*. London: Academic Press.
- MERRILL, M. C.** 1915: 'Electrolytic determination of exosmosis from the roots of plants subjected to the action of various agents'; In: *Annals of the Missouri Botanical Garden*, Vol. 2, p. 507–572.
- MICHAELIS, L.; MENTEN, M. L.** 1913: 'Die Kinetik der Invertinwirkung'; In: *Biochemische Zeitschrift*, Vol. 49, p. 333–369.
- NUSSAUME, L.; KANNO, S.; JAVOT, H.; MARIN, E.; POCHON, N.; AYADI, A.** 2011: 'Phosphate import in plants: focus on the PHT1 transporters'; In: *Frontiers in Plant Science* (Vol. 2), p. 1–12. Available online: <http://www.frontiersin.org/Journal/10.3389/fpls.2011.00083/full#B77>.
- PURVES, W. K.; SADAVA, D.; ORIANI, G. H.; HELLER, C.** 2006: *Biologie*. 7. Aufl. München: Elsevier.

- RAGHOTHAMA, K. G.** 1999: 'Phosphate acquisition'; In: *Annu. Rev. Plant Physiol. Plant Mol. Biol.* (50), p. 665–693.
- SANTNER, J.** 2011: *Mobility, transport and uptake of phosphorus in close proximity to plant roots.* Dissertation: *University of Natural Resources and Life Sciences, Wien.* Institute of Soil Science.
- SANTNER, J.; ZHANG, H.; LEITNER, D.; SCHNEPF, A.; PROHASKA, T.; PUSCHENREITER, M.; WENZEL, W. W.** 2012: 'High-resolution chemical imaging of labile phosphorus in the rhizosphere of *Brassica napus* L. cultivars'; In: *Environmental and Experimental Botany* (77), p. 219–226.
- SCHROEDER, D.** 1972: *Bodenkunde in Stichworten.* 2. Aufl. Kiel: Verlag Ferdinand Hirt.
- SMITH, F. W.; MUDGE, S. R.; RAE, A. L.; GLASSOP, D.** 2003: 'Phosphate transport in plants'; In: *Plant and Soil* (248), p. 71–83.
- ZANG, H.** 2003: *DGT – for measurements in waters, soils and sediments.* 2003. Skelmorlie, Quernmore, Lancaster.
- ZHANG, H.; DAVISON, W.** 1995: 'Performance characteristics of diffusion gradients in thin films for the in situ measurement of trace metals in aqueous solution'; In: *Anal. Chem.* (67), p. 3391–400.
- ZHANG, H.; DAVISON, W.; GADI, R.; KOBAYASHI, T.** 1998: 'In situ measurement of dissolved phosphorus in natural waters using DGT'; In: *Analytica Chimica Acta* (370), p. 29–38.
- ZHANG, H.; DAVISON, W.** 1999: 'Diffusional characteristics of hydrogels used in DGT and DET techniques'; *Analytica Chimica Acta* (398), p. 329.

6. Appendix

6.1. Method protocols

6.1.1. Soil fertilization protocol

Nutrient salt	addition to soil mg kg ⁻¹	addition to soil mg 6 kg ⁻¹	addition to all 4 treatments mg	salt in 250 ml mg
<i>a</i> NH ₄ NO ₃	181.1	1087	4347	5434
<i>b</i> KCl	124.5	747	2987	3734
<i>c</i> MgCl ₂ x 6H ₂ O	134.3	806	3222	4028
<i>d</i> ZnSO ₄ x 7H ₂ O	33.9	203	814	1017
<i>e</i> KH ₂ PO ₄	45.9	276	1103	1378
1)	prepare solutions		Treatments: Forchtenstein +P - P Santomera +P - P	
2)	weigh 4 soils, 6kg each			
3)	per treatment: +P 5 partitions in crucibles add solutions <i>a-e</i> (50mL) drying of soil partitions pulverize and mix back in	-P 4 partitions in crucibles add solutions <i>a-d</i> (50 mL)		
4)	Moistening oft he soils			

6.1.3. LA-ICP-MS standard preparation protocol

	P concentration $\mu\text{g cm}^{-2}$	F_t	time		P $C_{\text{soln}}/C_{\text{DGT}}$ $\mu\text{g L}^{-1}$	P -stock ml L^{-1}	P-stock for 3L mL	NaCl 1M mL
			seconds	hours				
Std 1	0.010	1	10800	3	15.6	0.048	0.144	30
Std 2	0.020	2	21600	6	15.6	0.048		
Std 3	0.040	1	10800	3	62.5	0.192	0.575	30
Std 4	0.080	2	21600	6	62.5	0.192		
Std 5	0.120	1.5	16200	4.5	125.0	0.383	1.149	30
Std 6	0.160	2	21600	6	125.0	0.383		
Std 7	0.200	2.5	27000	7.5	125.0	0.383		
D	$5.57\text{E}^{-06} \text{ cm}^2 \text{ s}^{-1}$							
A	3.1415 cm^2							
t	10800 s							
d_g	0.094 cm							

6.1.4. Hydroponics/Gelrite nutrient solution protocol

nutrient gel solution or hydroponic solution							
		stock	target in gel solution	addition	addition	addition	
mmol L ⁻¹	g mol ⁻¹	g L ⁻¹	g L ⁻¹	mL L ⁻¹	mL 100 mL ⁻¹	mL L ⁻¹	mL L ⁻¹
4	Ca(NO ₃) ₂ x 4H ₂ O	236.2	100	0.94	9.4	0.94	9.4
1.2	KNO ₃	101.1	100	0.12	1.2	0.12	1.2
1	MgSO ₄ x 7H ₂ O	246.5	100	0.25	2.5	0.25	2.5
2	MES	195.2	100	0.39	3.9	0.39	3.9
μmol L ⁻¹	g mol ⁻¹	mg L ⁻¹	mg L ⁻¹	mL L ⁻¹	mL 100 mL ⁻¹	mL L ⁻¹	mL L ⁻¹
25	NaCl	58.4	100	1.46	14.6	1.46	14.6
15	H ₃ BO ₃	61.8	100	0.93	9.3	0.93	9.3
10	Fe(III)EDDHA	360.4	100	3.60	36.0	3.60	36.0
5	MnSO ₄ x H ₂ O	169.0	100	0.85	8.5	0.85	8.5
1	ZnCl ₂	136.3	100	0.14	1.4	0.14	1.4
0.5	CuSO ₄ x 5H ₂ O	249.7	100	0.12	1.2	0.12	1.2
0.07	(NH ₄) ₆ Mo ₇ O ₂₄ x 4H ₂ O	1235.9	100	0.09	0.9	0.09	0.9

6.2. Calibration tables for the ³¹P-efflux experiments

F1R2 – Forchtenstein, P-fertilized

Table 8 shows the mean values of the ³¹P/¹³C ratio measured for F1R2 on the DGT standards by LA ICP-MS, their blank correction and the correlating phosphorus loadings according to the colorimetric analysis and the following conversion of the data. These data were used to calibrate the data measured on F1R2.

³¹ P/ ¹³ C Mean Values Blank Corrected and Correlating Standard Loadings			
Standard Name	³¹ P/ ¹³ C mean	³¹ P/ ¹³ C mean blank corrected	P µg cm ⁻²
1.1	0.0404	0.0325	0.0127
1.2	0.0364	0.0285	0.0182
1.3	0.0564	0.0485	0.0627
2.1	0.0951	0.0872	0.0480
2.3	0.161	0.153	0.0675
3.1	0.283	0.275	0.0968
3.3	0.373	0.365	0.145
3.5	0.354	0.346	0.225
B1	0.0101		
B2	0.00773		
B3	0.00591		
mean blank	0.00790		

By plotting the ³¹P/¹³C means against P loading per cm², the following calibration equation for F1R2 was obtained:

$$y = 0.4474x + 0.0098$$

$$R^2 = 0.8026$$

F2R1: Forchtenstein, P-unfertilized

Table 9 shows the mean values of the $^{31}\text{P}/^{13}\text{C}$ ratio measured for F2R1 on the DGT standards by LA ICP-MS, their blank correction and the correlating phosphorus loadings according to the colorimetric analysis and the following conversion of the data. These data were used to calibrate the data measured on F2R1.

$^{31}\text{P}/^{13}\text{C}$ Mean Values Blank Corrected and Correlating Standard Loadings			
Standard Name	$^{31}\text{P}/^{13}\text{C}$ mean	$^{31}\text{P}/^{13}\text{C}$ mean blank corrected	P $\mu\text{g cm}^{-2}$
1.1	0.0257	0.0213	0.0127
1.2	0.0249	0.0205	0.0182
1.3	0.0405	0.0361	0.0627
2.1	0.0589	0.0545	0.0480
2.3	0.113	0.108	0.0675
3.1	0.157	0.152	0.0968
3.3	0.275	0.271	0.146
3.5	0.239	0.235	0.225
B1	0.00476		
B2	0.00503		
B3	0.00343		
mean blank	0.00441		

By plotting the $^{31}\text{P}/^{13}\text{C}$ means against P loading per cm^2 , the following calibration equation for F2R1 was obtained:

$$y = 0.6466x + 0.0118$$

$$R^2 = 0.8058$$

S1R2: Santomera, P-fertilized

Table 10 shows the mean values of the $^{31}\text{P}/^{13}\text{C}$ ratio measured for S1R2 on the DGT standards by LA ICP-MS, their blank correction and the correlating phosphorus loadings according to the colorimetric analysis and the following conversion of the data. These data were used to calibrate the data measured on S1R2.

$^{31}\text{P}/^{13}\text{C}$ Mean Values Blank Corrected and Correlating Standard Loadings				
Standard	$^{31}\text{P}/^{13}\text{C}$ mean	$^{31}\text{P}/^{13}\text{C}$ mean blank corrected		P $\mu\text{g cm}^{-2}$
1.1	0.0349	0.0270		0.0127
1.2	0.0328	0.0249		0.0182
1.3	0.0500	0.0421		0.0627
2.1	0.0924	0.0845		0.0480
2.3	0.163	0.155		0.0675
3.1	0.249	0.241		0.0968
3.3	0.387	0.379		0.145
3.5	0.377	0.370		0.225
B1	0.00993			
B2	0.00746			
B3	0.00628			
mean blank	0.00789			

By plotting the $^{31}\text{P}/^{13}\text{C}$ means against P loading per cm^2 , the following calibration equation for S1R2 was obtained:

$$y = 0.4397x + 0.0118$$

$$R^2 = 0.8459$$

S2R1: Santomera, P-unfertilized

Table 11 shows the mean values of the $^{31}\text{P}/^{13}\text{C}$ ratio measured for S2R1 on the DGT standards by LA ICP-MS, their blank correction and the correlating phosphorus loadings according to the colorimetric analysis and the following conversion of the data. These data were used to calibrate the data measured on S2R1.

$^{31}\text{P}/^{13}\text{C}$ Mean Values Blank Corrected and Correlating Standard Loadings				
standard	$^{31}\text{P}/^{13}\text{C}$ mean	$^{31}\text{P}/^{13}\text{C}$ mean blank corrected		P $\mu\text{g cm}^{-2}$
1.1	0.0661	0.0403		0.0127
1.2	0.0385	0.0128		0.0182
1.3	0.0536	0.0279		0.0627
2.1	0.0798	0.0541		0.0480
2.3	0.144	0.118		0.0675
3.1	0.194	0.168		0.0968
3.3	0.318	0.292		0.145
3.5	0.272	0.247		0.225
B1	0.0351			
B2	0.0239			
B3	0.0183			
mean blank	0.0257			

By plotting the $^{31}\text{P}/^{13}\text{C}$ means against P loading per cm^2 , the following calibration equation for S1R2 was obtained:

$$y = 0.568x + 0.0142$$

$$R^2 = 0.7681$$

6.3. List of rhizotrons for the ³³P-efflux experiments

Rhizotron	P-Fertilization	Substrate	Fill weight g	Fill height mm	ρ g/cm ³	Spike μ L
R1	yes	Forchtenstein	663	368	0.0120	9
R2	yes	Forchtenstein	682	365	0.0124	9
R3	yes	Forchtenstein	671	366	0.0122	9
R4	no	Forchtenstein	665	368	0.0120	9
R5	no	Forchtenstein	657	364	0.0120	9
R6	no	Forchtenstein	658	367	0.0120	9
R8	no	Santomera	653	367	0.0119	3
R9	no	Santomera	688	371	0.0123	3
R10	yes	Santomera	627	364	0.0115	3
R11	yes	Santomera	653	368	0.0118	3
R12	yes	Santomera	638	363	0.0117	3
Rg	yes	Agargel	-	-		3
RA	yes	Agargel	-	-		15
RB	yes	Agargel	-	-		15
RC	yes	Agargel	-	-		15
RD	yes	Agargel	-	-		15

Rhizotron	Spike Activity $\mu\text{Ci}/\mu\text{L}$	Spike $\mu\text{Ci}/\text{Plant}$	Label date/time	DGT Sampling End
R1	2088	18800	11.09.13/16:40	13.09.13/14:35
R2	2088	18800	11.09.13/16:43	13.09.13/14:25
R3	2088	18800	11.09.13/16:45	13.09.13/14:15
R4	2088	18800	11.09.13/16:48	13.09.13/14:05
R5	2088	18800	11.09.13/17:01	13.09.13/13:55
R6	2088	18800	11.09.13/17:05	13.09.13/13:45
R8	6392	19200	31.07.13/16:15	02.08.13/14:40
R9	6392	19200	31.07.13/16:10	02.08.13/14:45
R10	6392	19200	31.07.13/16:05	02.08.13/14:50
R11	6392	19200	31.07.13/16:20	02.08.13/14:55
R12	6392	19200	31.07.13/16:25	02.08.13/15:00
Rg	6392	19200	31.07.13/16:30	02.08.13/15:05
RA	0.999	15000	07.10.13/13:15	09.10.13/11:35
RB	0.999	15000	07.10.13/13:17	09.10.13/11:41
RC	0.999	15000	07.10.13/13:19	09.10.13/11:49
RD	0.999	15000	07.10.13/13:20	09.10.13/11:55

Rhizotron	Plant Imaging Start	Plant Imaging End	DGT Imaging Start	DGT Imaging End
R1	13.09.13/14:50	13.09.13/16:50	13.09.13/15:05	16.09.13/13:40
R2	13.09.13/14:50	13.09.13/16:50	13.09.13/15:05	16.09.13/13:40
R3	13.09.13/14:50	13.09.13/16:50	13.09.13/15:05	16.09.13/13:40
R4	13.09.13/14:50	13.09.13/16:50	13.09.13/15:05	16.09.13/13:40
R5	13.09.13/14:50	13.09.13/16:50	13.09.13/15:05	16.09.13/13:40
R6	13.09.13/14:50	13.09.13/16:50	13.09.13/15:05	16.09.13/13:40
R8	02.08.13/15:10	02.08.13/17:05	02.08.13/15:10	05.08.13/13:30
R9	02.08.13/15:10	02.08.13/17:05	02.08.13/15:10	05.08.13/13:30
R10	02.08.13/15:10	02.08.13/17:05	02.08.13/15:10	05.08.13/13:30
R11	02.08.13/15:10	02.08.13/17:05	02.08.13/15:10	05.08.13/13:30
R12	02.08.13/15:10	02.08.13/17:05	02.08.13/15:10	05.08.13/13:30
Rg	02.08.13/15:10	02.08.13/17:05	02.08.13/15:10	05.08.13/13:30
RA	09.10.13/11:46	09.10.13/14:08	09.10.13/11:58	11.10.13/12:30
RB	09.10.13/11:46	09.10.13/14:08	09.10.13/11:58	11.10.13/12:30
RC	09.10.13/11:57	09.10.13/14:08	09.10.13/11:58	11.10.13/12:30
RD	09.10.13/11:57	09.10.13/14:08	09.10.13/11:58	11.10.13/12:30

6.4. Tables of root axis/root tip efflux ratios

The following tables show the calculation of the root axis to root tip efflux percentages of root segments of each scan picture:

R3	average [CPM/pixel]	area [pixels]	noise corrected signal [CPM]	signal [CPM/pixel]	axis/tip percentage
noise	108	23628			
root axis	157	439	21526	49	1.402%
root tip (efflux area)	603	177	87647	3506	
root axis	198	734	66177	90	0.960%
root tip (efflux area)	562	517	234743	9390	

R6	average [CPM/pixel]	area [pixels]	noise corrected signal [CPM]	signal [CPM/pixel]	axis/tip percentage
noise	111	7566			
root axis	180	886	61101	69	0.332%
root tip (efflux area)	1928	286	519876	20795	
root axis	145	638	21699	34	0.440%
root tip (efflux area)	875	253	193530	7741	

R8	average [CPM/pixel]	area [pixels]	noise corrected signal [CPM]	signal [CPM/pixel]	axis/tip percentage
noise	126	8455			
root axis	188	100	6226	62	0.100%
root tip (efflux area)	3243	501	1562109	62484	
root axis	149	150	3588	24	0.036%
root tip (efflux area)	2509	696	1658955	66358	
Main Root Axis A	301	76	8510	112	
Main Root Axis B	306	101	18258	181	
Main Root Axis C	205	325	25667	79	

R9	average [CPM/pixel]	area [pixels]	noise corrected signal [CPM]	signal [CPM/pixel]	axis/tip percentage
noise	131	7910			
root axis	250	277	33272	120	0.500%
root tip (efflux area)	2229	285	598029	23921	
root axis	269	360	50081	139	1.098%
root tip (efflux area)	781	486	316001	12640	
Main Root Axis A	227	246	23841	97	
Main Root Axis B	274	229	32934	144	
Main Root Axis C	207	182	13851	76	

R10	average [CPM/pixel]	area [pixels]	noise corrected signal [CPM]	signal [CPM/pixel]	axis/tip percentage
noise	138	8344			
root axis	200	152	9572	63	0.296%
root tip (efflux area)	2160	261	527853	21114	
root axis	170	315	10400	33	0.063%
root tip (efflux area)	3664	368	1297930	51917	
Main Root Axis A	153	827	12404	15	
Main Root Axis B	187	591	28984	49	
Main Root Axis C	224	349	30005	86	

R11	average [CPM/pixel]	area [pixels]	noise corrected signal [CPM]	signal [CPM/pixel]	axis/tip percentage
noise	122	8866			
root axis	133	621	7003	11	0.796%
root tip (efflux area)	268	242	35409	1416	

R12	average [CPM/pixel]	area [pixels]	noise corrected signal [CPM]	signal [CPM/pixel]	axis/tip percentage
noise	136	11233			
root axis	172	291	10777	37	0.294%
root tip (efflux area)	1133	313	312295	12492	
root axis	148	545	7088	13	0.170%
root tip (efflux area)	736	317	190234	7609	
Main Root Axis A	220	185	15687	85	
Main Root Axis B	312	144	25485	177	